MEASUREMENT OF OPERATING TEMPERATURE IN SPARK IGNITION ENGINE

by

DAVID D. CHUA-UNSU

B.S.M.E., Mapua Institute of Technology
(Manila, Philippines 1956)

B.S.E.E., Mapua Institute of Technology
(Manila, Philippines 1957)

SUBMITTED IN PARTIAL FULFILLMENT
OF THE REQUIREMENTS FOR THE
DEGREE OF MASTER OF
SCIENCE

AT THE

MASSACHUSETTS INSTITUTE OF TECHNOLOGY
February, 1959

Signature of Author .....
Department of Mech. Eng., Feb. 26, 1959

Certified by .....
Thesis Supervisor

Accepted by .....
Chairman, Departmental Committee
on Graduate Students

Cambridge, Massachusetts
February 26, 1959

Professor Warren M. Rohsenow, Chairman
Departmental Committee on Graduate Students
Massachusetts Institute of Technology
Cambridge, Massachusetts

Dear Professor Rohsenow:

I hereby submit a thesis entitled "Measurement of Operating Temperature in Spark Ignition Engine" submitted in partial fulfillment of the requirements for the degree of Master of Science in Mechanical Engineering.

Respectfully yours,

David D. Chua-unsu

MEASUREMENT OF OPERATING TEMPERATURE IN SPARK IGNITION ENGINE

BY

David D. Chua-unsu

Submitted to the Department of Mechanical Engineering on February 26, 1959 in partial fulfillment of the requirement for the degree of Master of Science in Mechanical Engineering.

ABSTRACT

The sound velocity method for instantaneous temperature measurement in the end gas region of a spark ignition engine is described. Curves of tip temperature measured by thermocouples and end gas temperature measured by sound velocity method at various gage length of the coupling rod and at different material of coupling rod, respectively, were calculated and plotted. The details of operation and conversion of data are given.

End gas temperature in motoring and firing runs are reported. The effect of using different materials for the coupling rods in the transducer on the temperature measurement are discussed. The effect of varying the gage length of the transducer bar on the temperature measurement are being discussed too.

Thesis Supervisor: Professor C. F. Taylor
Title: Professor of Mechanical Engineering

ACKNOWLEDGEMENT

The author wishes to express his sincere thanks to those whose contribution to this work is far beyond words here can describe.

Professor C. F. Taylor, who acted as thesis supervisor and gave many valuable suggestions besides guidances and inspiration.

Mr. J. C. Livengood, Mr. C. Talbot and Professor Rogowski, whose personal help and encouragement are most deeply appreciated.

The staff of Sloan Automotive and Aircraft Engine Laboratory of M.I.T., who helped in every way to make the project successful.

TABLE OF CONTENTS

TABLE OF CONTENTS

TABLE OF CONTENTS

INTRODUCTION

The need of instantaneous and continuous temperature data throughout the combustion process in internal-combustion engines has long been recognized. Combustion rates, chemical equilibria, fuel vaporization, ignition lag, and heat transfer are all affected by temperature. It was expected that knowledge of such temperature would shed important light on questions of charge density-volumetric efficiency, composition-residual gas percentage, and combustion-flame speed and knock.

The measurement of the instantaneous gas temperature inside the combustion chamber of a spark ignition engine is a difficult task, due to the extremely high rate of temperature change, the wide range of temperature encountered and the large temperature gradient. Even in motored engines, or before the charge is ignited in firing engines, there is non-uniformity of temperature so that perfect gas law can only give an average reading but not the temperature of the portion in question. Therefore the instrument developed for this purpose must be accurate over the whole range of temperature, able to measure the local temperature at the point of interest, and must have a response fast enough to follow the high rate of temperature change.

The temperature of the unburned gas in an engine, especially that of the "end gas" or the last part of the charge to burn, is of great interest. This region is the last to be consumed by the flame front. The unburned mixture in this region has experienced a history of induction, mixing with residuals, heat transfer, compression by the piston, and a further elevation in temperature and pressure by the earlier burning portions of the charge. It is also

in this region where detonation or "knock" reactions occur. Therefore, it is quite desirable to develop a suitable method to measure the instantaneous temperature of the end gas region.

The study of possible techniques to measure instantaneous end gas temperature in engines were four: (Ref. 1)

a) Thermocouple technique,
b) Absorption method,
c) Infrared radiation method, and
d) Sound velocity method

The author uses the sound velocity method in the temperature measurement of the spark ignition engines since it has been designed and developed here at M.I.T. and the apparatus is available for the project.

The sound velocity method is based on the relation

$$a^2 = kRT \qquad (1)$$

where a = velocity of sound,
k = specific heat ratio, = c_p/c_v
R = perfect gas constant,
T = absolute temperature

This equation relates the velocity of small wave propagation in a perfect gas to its temperature. By measuring the velocity of sound wave in the end gas at a certain point of the cycle, the instantaneous temperature can be determined, with some knowledge and reasonable assumption about the composition and properties of the end gas.

The sound velocity method involves transmitting an acoustical impulse through a gas path of known length and

measuring the time of propagation through the gas. Such a measurement will yield a value for the average velocity of sound in the path.

By varying the gage length of the transducer bars, we try to optimize the gage length and find out its effect on the temperature measurement. We also try to find the ideal length that will yield a less error in the sound velocity method in temperature measurement. The works also cover the varying of the materials used for the transducer bars and find out its effect on the temperature measurement.

SECTION I

THE TEST ENGINE AND INSTRUMENTATION

ENGINE SPECIFICATIONS:

The engine used is a modified CFR single cylinder spark ignition engine with a variable-compression ratio cylinder barrel and a removal head. Between the head and the cylinder is a "sandwich" formed by three steel plates. The space enclosed in this "sandwich" between the piston and the cylinder head forms the combustion chamber. Figure 1 show the combustion chamber used, it is a open chamber.

The dimensions and specifications of the engine are:

Manufacturer:	Waukesha Motor Company
Bore	3-1/4 inches
Stroke	4-1/2 inches
Compression ratio	Variable, approximately 3 to 6.
Displacement	37.33 cubic inches
Connecting rod	10 inches long (center to center)
Inlet valve lift	0.265 inch at 0.008 inch valve clearance
Valve port diameter	1.187 inches
Combustion chamber	Special
Piston	Special
Spark Plug	Special, 1/4" spark plug

Figure 3 show the engine set up used. The engine is connected to a dynamometer of the eddy current type with an absorbing capacity of 50 horsepower and a cranking a.c. motor of 10 horsepower. Fuel and air are metered separately and mixed in a heated tank before entering the inlet port. Inlet and exhaust pressures can be controlled by the super-charged and vacuum pumps in the laboratory. The inlet,

jacket, and oil temperature can be controlled with steam and cooling water in heat exchangers.

ENGINE INSTRUMENTATIONS:

The engine speed was indicated by two means: an electric tachometer giving the approximate rpm and a stroboscope flashing at 60 cps indicating the exact hundred-rpm when the white paint markers on every other 5 degrees on the flywheel appear to stand-still.

The inlet and exhaust pressures were measured at the inlet and exhaust tanks by mercury manometers. The inlet temperature is measured at the entrance to the inlet port with a thermometer. The jacket and oil temperature were both measured by thermometers too.

The air flow was measured by an A.S.M.E. orifice meter. (Ref. 9) The orifice has a diameter of 0.515 inch. For this meter, the air flow in lb/sec is calculated by

$$w = 0.0182 \sqrt{P_o \Delta p / T_o} \qquad (2)$$

where w = air flow in lb/sec
P_o = pressure before orifice in inches of mercury,
T_o = temperature before orifice in degree Rankine,
Δp = pressure drop across orifice in inches of water.

For convenient, a chart of Δp against w were plotted for P_o and T_o. A correction factor was used for a measured pressure and temperature at a certain standard. P_o is 29.92 inches of mercury and T_o is 518.4°R. The correction factor is

$$CF = \sqrt{(P/29.92)(518.4/T)} \qquad (3)$$

Therefore,

$$w_a = w(CF) \qquad (4)$$

where w_a is the actual air flow.

The fuel flow was measured by a calibrated rotameter. Calibration curve was obtained as shown in Figure 26.

The brake torque of the engine was measured by a hydraulic scale which indicates the scale load on a mercury manometer.

A protractor disc with 1 degree crank angle marks mounted concentric with the crankshaft was used to indicate the position of the spark, the time of triggering of sound signal in the sound velocity method, and the time at which the flame front passed an ionization gap.

The cylinder pressure was studied with the M.I.T. balanced pressure point-by-point indicator. (Ref. 10) The indicator is used with a free-diaphragm pickup unit. The free-diaphragm unit has the advantage of being unlikely to give a constant error in pressure as the clamped-diaphragm units often do. The indicator cards were all taken with a 100 psi per inch spring, and the maximum error about $\pm$ 1%.

ENGINE CONDITIONS:

All the data were taken after the engine had been running steadily at a set of conditions for at least 10 to 15 minutes or more.

The speed of the engine could easily be maintained exactly at the desired value during data taking. The speeds used were 1000 and 2000 rpm.

The inlet, oil and jacket temperatures were maintained at 160, 150 and 180 degrees Fahrenheit respectively in all the runs. They were maintained within ± 2°F during data taking.

The inlet pressure and exhaust pressure could be maintained within ± 0.1 inch mercury of the desired value. Inlet and exhaust pressures were maintained at 28 inches of mercury and 31 inches of mercury respectively in all the runs.

The fuel rate could be set quite accurately. The variation was less than 1%. The fuel-air ratio was maintained at 0.08 in all the runs. Iso-octane was used for its stability, anti-knocking quality, absence of pre-flame reactions, etc. .

The engine valve clearance were set at 0.006 inch and 0.025 inch at standstill for inlet and exhaust valves respectively.

The engine is running at a spark advance that would give the best power.

TAKING INDICATOR CARDS:

Simultaneous with the reading of sound velocity over the cycle, one or more indicator cards for each run were taken. The M.I.T. balanced pressure indicator was used. A 100 psi per inch spring with a free-diaphragm pickup unit were used in all the runs. A sample indicator is shown in Figure 2.

VARIABLES INVESTIGATED:

The engine conditions were maintained constant in all the runs. The only variable considered were:

a) Gage length of the coupling rods. Sizes of 1/8, 1/4, 1/2 and 5/8 inch were being used and they were all made of brass. They were measured both by sound velocity method for the gas temperature and by thermocouple for the tip temperature. The effect of varying the gage length on temperature measurement were to be investigated.

b) A fixed gage length of 1/4 inch were used. The variable were the material of the coupling rods. Stainless steel and brass were being used and the effect of materials of coupling rod on temperature measurement were to be investigated.

SECTION 2

THE SOUND VELOCITY METHOD

THEORETICAL FOUNDATION:

For practical purposes and as far as the present measurement problem is concerned, it can be stated that the sound velocity method is convenient to measure engine gas temperature between 450 and 2000°R within a few tens of microseconds. Also, measurements can be made in hot, burned products of combustion at temperature in excess of 4000°R, but the accuracy of these measurements is not yet established, since it gives quite a scatter.

We can called the propagation to be linear if:

a) the propagating medium acts as a perfect gas,

b) the pressure and temperature changes caused by the sound are negligible, and

c) the sound excitation is a pure sinusoidal pressure change at each point in the propagation path.

The propagation velocity is defined by

$$a^2 = K_e / \rho \tag{5}$$

and

$$K_e = c_p K_t / c_v = kv(-\partial p/\partial v) \tag{6}$$

but

$$-\partial p \Delta v = \frac{m}{M} \bar{R} T \frac{1}{v^2} \tag{7}$$

Therefore,

$$a^2 = kv \frac{m\bar{R}T}{M} \frac{1}{\rho v^2}$$

$$a^2 = kRT \tag{8}$$

where K_e = Iso-entropic stiffness
K_t = Isothermal stiffness
a = propagation velocity of sound
$k = c_p/c_v$ = specific heat ratio
v = volume

p = pressure
$\bar{R}$ = perfect gas constant
$R = \bar{R}/M$
m = mass
M = molecular mass
ρ = specific mass

The velocity of sound a is a function of the thermodynamics coefficients, molecular constants and absolute temperature T only and its measurement can be therefore used to determine the temperature of any gas if the other constant are known.

Thus the determination of gas temperature by sound velocity method envolves:

1) the measurement of sound velocity in the gas, and
2) the determination of the value of kR to be used.

A scheme of direct measurement by employing the gage length and transit time is used in measuring the sound velocity in the end gas. A transient sound pulse is generated and detected inside the test chamber. The transit time is defined as the interval between corresponding points of the transmitted and detected signal and is measured by means of calibrated electronic circuits. The simultaneous knowledge of the transmission gage length and of the transit time yields the velocity of sound. And the temperature can be calculated by using the value of kR and equation (8).

PRINCIPLE OF OPERATION:

The schematic arrangement of the apparatus used for sound velocity measurement in the end gas is shown in Figure 5.

The breaker BR on the engine distribution shaft makes a contact every complete engine cycle (2 revolutions). The timing of the contact can be manually adjusted to any position of the engine cycle.

As a contact is made by the breaker, the synchronizer SY sends a square pulse to the synchroscope which in turn sends out a triggering pulse to the transmitter circuit TR. The transmitter at the time $t_o = 0$, then provides a driving pulse voltage to the transmitting crystal, XTR. On receiving the electric impulse, the crystal sends an acoustic "signal" through the coupling rod, CR1. This signal is propagated from the end of the transmitting rod through the gas path to the receiving rod, CR2. It travels through the receiving rod and generates an electric voltage in the receiving crystal, SRC. This voltage is picked up and amplified by the receiver circuit, RC, which is directly connected to the A-R scope signal input, delay however by the receivers own delay t_{Rc} . The calibrated delay circuit PO of the synchroscope is used for transit time determination.

The "received" pulse comes back to the synchroscope after some delay around the entire path. This delay includes the time taken from the synchroscope to the transmitting crystal, the time for the acoustic signal to travel through the coupling rods, and the time for the acoustic signal to go across the gas path. The length of the gas path is called the gage length. The delay from the input of the square pulse send by the synchronizer to the start of transmission across the gas path is of the order of 30 micro-seconds and is assumed to be constant while the gas path varies. The gas path delay is the transit time of interest. The gage length divided by the transit time gives the velocity of sound in the gas.

The start of the synchroscope trace across the screen can be delayed after the pulse input. The delay time is controlled by a high precision delay circuit and can be adjusted by a calibrated potentiometer, PO. When the potentiometer is adjusted so that the start of the synchroscope trace coincides with the first rise due to the received signal, the potentiometer dial reading represents the total delay as the signal goes around the entire path. A signal travelling through a gas path of one temperature or composition will give one reading for total delay, and one travelling through a gas path of different temperature or composition will give a different reading. The difference in transit time in the two cases can be obtained by taking the total delay readings and subtracting one from the other.

Therefore, if some known gas at an accurately known temperature is introduced between the sound transmitting and receiving surfaces, the gas path delay can be calculated from the known gage length and sound velocity. This procedure is called the reference calibration. A dial reading for this gas is taken. Then when a gas with known composition but unknown temperature is between the gage, a dial reading can again be taken, and the difference in transit time can be calculated. Knowing the first transit time, the unknown transit time can be obtained by subtraction. The sound velocity in the gas of unknown temperature is obtained by dividing the gage length by the transit time. With the aid of a sound velocity vs. temperature curve for this gas, its temperature can be found. Appendix I will show how those working curve were obtained. Figures 13-A, 13-B and 14 shows those curves.

COMPONENT OF THE SOUND VELOCITY APPARATUS:

1.) Mechanical Arrangement:

a) Combustion Chamber

- In order to have a well defined end gas and to apply the sound velocity measuring device, a special combustion chamber was designed to fit the laboratory engine. It is made by "sandwich" construction with gaskets between the steel members to reduce the transmission of sound energy via this path from transmitter to receiver.

b) Piston and Piston Rings:

- The piston was specially designed with a crown to block off the back part of the combustion chamber as can be seen in figure 1. This reduces the clearance volume, and should make the flame to spread from the spark plugs toward the front of the chamber, and the charge in the end cavity should be the last part to burn.

  For minimum leakage and oil control in both motoring and firing runs, the piston was made with five compression rings and two oil rings. A low heat expansion coefficient alloy was used as material.

c) Coupling rods:

- Brass coupling rods which provide the mechanical link between the barium titanate crystals and the inner surface of the test zone, are clamped into position as shown in figure 5 and are provided with additonal acoustical isolation for the purpose of interrupting alternate path transmission through the metal parts. Figures 4 and 6 show the different sizes of coupling rods used.

2.) Electronic Apparatus:

a) The synchronizer:
- To determine the point in the engine cycle at which the measurement is to be performed, a synchronizer is used. This can be any electrical signal controlled by the engine crank or other shaft.

b) The trigger:
- The trigger, which initiates the electrical pulse driving the sound generator. The pulse provided by the trigger is of the DuMont 256-F oscilloscope has been used.

c) The pulser, driven by the trigger:
- A hydrogen thyratron (3C45) is suitable because of short rise time and accurate triggering. The grid is maintained around -50v in absence of trigger. The plate voltage is adjusted between 0 to 3000 volts, for practical purposes, however, the plate voltage has been consistently limited to 1600 volts.

d) The crystal transducers:
- They are longitudinally excited disks of barium titanate with fired-on electrodes and a natural frequency of about 2 to 2.5 Mcps (mega-cycle per second). Figure 4 shows the crystal transducer.

The above component composed the sound generator or transmitter. Figure 7 show the circuit diagram of the transmitter.

The output voltage is limited only by the ability of the transducer crystals to withstands the peak voltages. Breakdowns have often occurred when the plate voltage of the output stage was in excess of 2200 volts. In addition,

little actual increase in the signal power was obtained with voltage above 1600 volts. Therefore, in the used of the electronic equipment, the voltage is always keep below 1600 volts.

e) The Receiver:

- The receiver is a low-noise, high-gain control and a marker generator. The noise figure is kept low by means of the grounded-cathode triode-grounded grid triode arrangement. A stabilized power supply and thorough shielding are employed. Figure 8 show the circuit diagram for the receiver.

f) Synchroscope - time measuring device:

- The time interval is measured by means of a calibrated sweep oscilloscope (DuMont 256-F). The trigger pulse generated by this synchroscope starts the acoustical signal in the sound generator and, at the same time, triggers the scope sweep. This sweep is delayed through a calibrated circuit so that the sweep on the CR screen will start at an arbitrary adjusted time interval after the trigger. The received (or its translation in a marker pulse) is connected to the vertical edge coincides with the sweep origin, the value indicated on the delay calibrations is equal to the transit time of the electro-acoustical signal, which includes all the electrical time lags introduced by the trigger, generator and receiver circuits.

  The synchroscope used is a type 256-F, A-R scope, DuMont made. This scope does two things in response to the signal:

  1) It starts the operation of a "delay circuit",
  2) It concurrently sends out a pulse which "fires" the transmitting circuit.

It has the following features:

1) Output trigger 100 volts, rise time less than 0.05 second, used to trigger the transmitter.
2) Video amplifier, 300 cps to 10 Mcps to 6 db.
3) Calibrated sweep (A-sweep) three ranges with speeds from approximately 30 micro-seconds per inch to 1125 micro-seconds per inch.
4) Expander and calibrated delays (R-sweep), the sweep speed can be increased by factors of 5, 10, and 25 to give rates of 1.2, 3, 6, 12, 30 and 60 micro-seconds, per inch. Calibrated delays are available on all R-sweep.

Figure 9 show the electronic equipment used.

CURVES OF SOUND VELOCITY VS TEMPERATURE:

In order to calculate and convert the measured sound velocity into temperature, the curves of sound velocity vs temperature should be used. Appendix I will show how those working curves were being obtained.

These sets of curves were used in converting sound velocity data into temperature. The percent residuals in the runs were estimated, based on a comparison with a few runs in which the residual percentage were calculated by the methods to be described in Appendix II.

OPERATING PROCEDURE:

In order to avoid any change in the electronic instruments due to insufficient warmup, all the electronic circuits were turned on at least half an hour before any

reading was taken. It was observed that after the equipment was well warmed up, there was no drifting in many hours.

The reading before the run starts (with air at known temperature and pressure in the gas path) is called the reference reading. Its accuracy has great importance on the accuracy of the temperature measurements. Therefore, every precaution for preventing error in the reference reading was taken. Since the signal was small at atmospheric pressures due to poor acoustic power transmission in the poorly matched system of brass bar and low density air, it was found desirable to increase the air density while taking the reference reading. Since pressure has no effect on the sound velocity in the range of operation, compressed air up to 100 psia was used to charge the cylinder when the engine was standing still with everything at room temperature. The highest sweep rate of the scope was used to give an expanded time scale. The internal triggering was used. The calibrated delay potentiometer was then adjusted until the first rise of the received signal coincides with the start of the sweep. The dial reading and the air temperature were recorded.

The cooling water on the coupling rods was turned on with the same flow rate in all the runs. This would equalize the effect on cooling the rods in different runs. A test during which the temperature of the brass bars was changed showed no detectable effect on the sound velocity reading. Figure 10 show a details of a transducer and figure 11 show the transducer mounted on the cylinder head.

A position-indicating circuit was connected to the breaker. This circuit included a thyratron operated spark generator which produces a spark at a spark plug when the signal from the breaker was fed into the circuit. The timing of the spark was indicated by the flashing of a neon

light on the crankshaft through a slit in a cover plate and the crank position at which the light flashed was read from a stationary protractor disc concentric with the crankshaft. A selector switch connected the breaker either to the position-indicating circuit or to the triggering circuit of the synchroscope.

To take data, the breaker was first set to the desired crank angle. The selector switch was then turned to the reading side so that the breaker started to trigger the pulse generating circuit. The delay potentiometer dial was turned until the beginning of the received signal coincides with the start of the sweep. The dial reading was recorded.

Reading were taken at different crank angles along the part of the cycle of interest.

When a set of dial readings and crank angles was recorded, the following steps were employed to get the temperature:

1) Determine the gas path delay at reference temperature by dividing the known gage length by the sound velocity in air at that temperature.
2) Determine the delay in the circuit other than the gas path by subtracting the gas path delay at reference temperature from the total delay reading from the dial at reference point.
3) Subtract the result of step 2 from the readings obtained at various crank angles to give the gas path transit time at each measurement.
4) Divide the gage length by the transit time to obtain the sound velocity.
5) Used the sound velocity vs. Temperature curves to obtain the temperature.

The choice of the correct curve to use involves a knowledge of this fuel-air ratio and the residual percentage. The fuel-air ratio is easily obtainable from the air and fuel flow measurements, but the residual content is more difficult to determine. Prior to this time, the residual percentage has been either arbitrarily assumed or estimated by means of fuel-air cycle calculations. These methods are not very satisfactory. See Appendix II for the calculation of residual content.

Since the residuals do not have a large effect on sound velocity, especially in a lean mixture, an assumed estimates of 10 to 15% can well serve the purpose of helping the selection of the appropriate sound velocity vs. temperature curves.

SECTION 3

RESULTS AND DISCUSSIONS

GENERAL SCHEME:

In all the runs made, the engine condition were maintained at a predetermined value that will give a good engine performance. (Refs. 2, 3, 4, 6, 7, 8) The only variable was the speed. The engine condition was:

Fuel - Iso-octane
Spark advance - BPSA*
Inlet temperature, T_i - 160°F
Jacket temperature, T_j - 180°F
Oil temperature, T_o - 150°F
Exhaust pressure, P_e - 31 inches of mercury abs.
Inlet pressure, P_i - 28 inches of mercury abs.
Fuel-air ratio, F = 0.08
Compression ratio, r - 6

For the investigation of the bar tip temperature by thermocouple and end gas temperature by sound velocity method, the following runs were made and plotted into curves in the following figures:

I. Figure 15

a) 0.598" Gap

Speed	Runs
1000 rpm - F**	5, 43, 52
1000 rpm - M***	10, 53, 56
2000 rpm - F	17, 55
2000 rpm - M	11, 54

---

* BPSA - best power spark advance
** F - firing
*** M - motoring

b) 0.476" Gap

Speed	Runs
1000 rpm - F	25
1000 rpm - M	24
2000 rpm - F	22
2000 rpm - M	23

c) 0.230" Gap

Speed	Runs
1000 rpm - F	26
1000 rpm - M	27
2000 rpm - F	29
2000 rpm - M	28

d) 0.102" Gap

Speed	Runs
1000 rpm - F	33, 35, 39, 51
1000 rpm - M	32, 34, 42, 50
2000 rpm - F	30, 36, 41, 49
2000 rpm - M	31, 37, 40, 48

II. Figure 16

Speed	Runs
2000 rpm - F	64, 68, 76, 79
1000 rpm - F	70, 74, 78, 89
2000 rpm - M	75, 82, 87, 92
1000 rpm - M	73, 85, 90, 95

III. Figure 17, 1000 rpm Motoring

Gap	Runs
0.598"	73, 105
0.476"	91, 95
0.230"	86, 90
0.102"	81, 85

IV. Figure 17-A, 0.102" Gap, 1000 rpm Motoring - Runs 85, 81, 77

V. Figure 18, 2000 rpm Motoring

Gap	Runs
0.598"	75
0.476"	92
0.230"	87
0.102"	82

VI. Figure 19, 1000 rpm Firing

Gap	Runs
0.598"	74
0.476"	70
0.230"	89
0.102"	78

VII. Figure 20, 2000 rpm Firing

Gap	Runs
0.598"	76
0.476"	64
0.230"	68
0.102"	79

VIII. Figure 21

Gap	1000 rpm - F	2000 rpm - F
0.598"	74	76
0.476"	70	64
0.230"	89	68
0.102"	78	79

IX. Figure 22 Runs 111, 112, 113, 114

X. Figure 23 Runs 120, 121, 127, 129

XI. Figure 24 Runs 122, 123, 128, 130

The runs listed above are the productive runs only, many other runs were made, but found unacceptable or were used as trial runs to get the engine and auxiliaries under normal operating conditions.

The bar tip temperature were measured directly by means of thermocouple. The temperatures of the end gas were computed from the gap transit at various crank angles before and after top center, for unburned and burned gases. The result of these computation were plotted in the graphs just mentioned above.

In all the experiments, performed to determined the effect of varying the gas path on temperature measurement, the transducer configuration used was that shown in figure 1. The horizontal bar was not changed, the four straight "vertical" bars of different tip length were used. These were made in pairs one for sound velocity measurements, the other drilled for a thermocouple soldered to the tip for tip temperature measurement. The four bar length used gave gas path length of 0.102, 0.230, 0.476, 0.598 inch, respectively. These arrangement were tested at two speed,

1000 and 2000 rpm with the engine motoring with air, and at the same speeds with the engine firing. The results are summarized in Figure 15 to 24.

SAMPLE CALCULATIONS OF END GAS TEMPERATURE BY SOUND VELOCITY METHOD:

RUN 85:

Reference Point:

Sweep delay =51 usec*
Air (room) temperature = 79°F (539°R)
Air pressure = 25 psig (2.7 atm. abs.)
Gage length, L = 0.102" = 0.0085 ft.

a° = 1138.2 ft/sec (from figure 13-B)
a°/a = 0.9994 (from figure 12)
a = 1138.2/0.9994 = 1138.9 ft/sec
t = L/a = 0.0085/1138.9 = 7.46 usec
Fixed delay = 51.00 - 7.46 = 43.54 usec

Engine Conditions:

Speed - 1000 rpm Motoring
Barometer reading - 763.8 mm Hg.
P_i = 28 inches of mercury P_e = 31 inches of mercury
T_i = 160°F T_j = 180°F
T_o = 150°F r = 6
Δp = 3.75 inches of water

From figure 25
w = 0.00825 lb/sec of air
$CF = \sqrt{(P/29.92)(518.4/T)}$
$= \sqrt{(30.02/29.92)(518.4/539)}$
$= 0.9844$
$w_a = w(CF) = 0.00825\ (0.9844) = 0.0081$ lb/sec of air

---

* usec = micro-seconds = 10^{-6} second

TABLE I

θ (deg)	Reading (usec)	usec[1] (10^{-6} sec)	a[2] (fps)	P[3] (atm.abs)	a°/a[4]	a° (fps)	T[5] (°R)
301	49.68	6.14	1384.4	2.18	0.9992	1383.3	800
306	49.55	6.01	1414.0	3.30	0.9990	1413.0	838
311	49.50	5.96	1436.2	3.60	0.9988	1435.0	858
316	49.33	5.85	1453.0	4.15	0.9975	1449.4	881
321	49.27	5.73	1482.0	4.70	0.9970	1478.2	918
326	49.20	5.66	1501.8	5.45	0.9968	1497.0	942
335	49.10	5.56	1528.8	6.05	0.9965	1523.0	978
336	49.02	5.48	1551.1	6.95	0.9960	1544.9	1007
341	48.97	5.43	1565.4	7.35	0.9955	1558.4	1025
346	48.90	5.36	1585.8	8.70	0.9950	1577.9	1052
351	48.86	5.32	1593.2	9.25	0.9950	1585.0	1065
357	48.81	5.27	1606.8	9.60	0.9945	1597.9	1080
360	48.82	5.28	1609.8	9.65	0.9945	1600.9	1084
3	48.81	5.27	1610.2	9.65	0.9945	1601.1	1085
8	48.88	5.34	1591.8	9.50	0.9950	1583.8	1059
13	49.00	5.46	1556.8	9.20	0.9950	1549.0	1012
18	49.02	5.48	1551.1	8.45	0.9955	1544.1	1005
23	49.15	5.61	1515.2	7.62	0.9960	1509.1	958
28	49.22	5.68	1496.5	6.60	0.9962	1490.8	934
33	49.37	5.83	1458.0	5.80	0.9968	1452.0	884
38	49.49	5.95	1429.0	5.10	0.9970	1424.4	850
43	49.66	6.12	1388.0	4.63	0.9973	1383.3	800
48	49.81	6.27	1355.7	4.00	0.9985	1353.7	765
53	49.90	6.36	1335.2	3.55	0.9989	1332.0	740
58	50.02	6.48	1211.7	3.26	0.9991	1310.5	716

(1) usec =reading - fixed delay

(2) a = L/usec

(3) P, obtain from the P-θ indicator card

(4) a°/a, from figure 12

(5) T, from figure 13-A

RUN 74

Reference Point:

Sweep delay = 84.78 usec
Air (room) temperature = 78°F (538°R)
Air pressure = 40 psig (3.7 atm. abs)
Gage length, L = 0.599" = 0.0499167 ft.

a° = 1137.2 ft/sec (from figure 13-B)
a°/a = 0.9972 (from figure 12)
$a = 1137.2/0.9972 = 1140.4$ ft/sec
$t = L/a = 0.0499167/1140.4 = 43.77$ usec

Fixed delay = 84.78 - 43.77 = 41.01 usec

Engine conditions:

Speed - 1000 rpm Firing
Barometer reading - 759.37 mm Hg.
P_i = 28 inches of mercury absolute
P_e = 31 inches of mercury absolute
T_i = 160°F T_j = 180°F
T_o = 150°F F = 0.08
r = 6 Δp = 3.9 inches of water
rotameter reading = 4.3 S.A.* = 35°BTC**

From figure 25,
w = 0.00865 lb/sec of air
$CF = \sqrt{(29.85/29.92)(518.4/538)} = 0.9813$
$w_a = w(CF) = 0.00865(0.9813) = 0.00848$ lb/sec of air

From figure 26,
$w_f = 0.68 \times 10^{-3}$ lb/sec of Iso-octane
$F = 0.68(10^{-3}) / 0.00848 = 0.0801$

---

* S.A. - spark advance
** BTC - before top center

TABLE II

θ (deg)	Reading (usec)	usec (10^{-6} sec)	a (fps)	P (atm.abs)	a°/a	a° (fps)	T (°R)
320	74.10	33.09	1509	4.53	0.9970	1504	1042
325	73.70	32.69	1528	5.06	0.9970	1523	1073
330	73.25	32.24	1548	5.67	0.9965	1547	1103
335	72.80	31.79	1570	6.26	0.9960	1562	1134
340	72.35	31.34	1591	7.20	0.9955	1585	1170
345	71.90	30.89	1616	9.00	0.9952	1609	1206
350	71.40	30.39	1640	10.33	0.9950	1633	1253
355	70.90	29.89	1670	12.72	0.9930	1659	1287
360	70.00	29.09	1716	15.56	0.9920	1700	1364
5	69.70	28.69	1740	19.67	0.9905	1723	1397
10	69.20	28.19	1770	23.94	0.9890	1749	1445
15	6.8.80	27.79	1796	25.90	0.9880	1772	1489

θ (deg)	Reading (usec)	usec (10^{-6} sec)	a (fps)	T * (°R)
15	56.60	15.59	3201.8	4665
20	56.60	15.59	3201.8	4665
25	56.70	15.69	3181.4	4595
30	56.90	15.89	3141.4	4465
35	57.20	16.19	3083.2	4280
40	57.30	16.29	3064.3	4220

* Figure 14 was used to obtained the burned gas temperature

EFFECT OF SPEED:

Under the conditions of the runs shown in figures 15 to 24, an increase in speed cause an increase in end gas temperature. This is caused by two effects:

1. There is a reduction in heat loss per unit mass as speed increases, due to the shortened time for heat transfer.

2. There is an induction work effect which will cause an increase in compression temperature. The temperature of the charge is lowered by the work done on the piston during the inlet stroke. As speed increases, this work decreases, due to increasing pressure drop through the inlet valve, This effect is probably considerably more important than the heat loss effect.

EFFECT OF TEMPERATURE GRADIENT:

$$a^2 = kRT_{sv} \qquad (8)$$

$$a = C\sqrt{T_{sv}} \qquad (9)$$

where $C = \sqrt{kR}$ = constant

a = sound velocity

k = specific heat ratio, $= c_p/c_v$

R = perfect gas constant,

T_{sv} = absolute temperature measured by sound velocity.

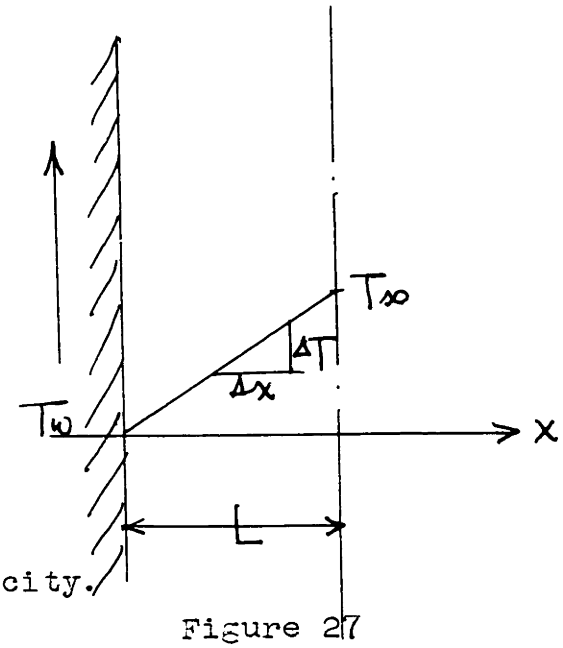

Figure 27

Assume the temperature gradient is linear and constant. From figure 27, we have

$$b = \Delta T/\Delta x = \frac{T_\infty - T_w}{L} \qquad (10)$$

where T_∞ = temperature of gas at free stream,
T_w = temperature of wall or tip temperature.

Therefore,

$$a = C(T_w + bx)^{1/2} \tag{11}$$

t = transit time

$$= \frac{\text{distance}}{\text{velocity}}$$

$$dt = \frac{dx}{C(T_w+bx)^{1/2}}$$

$$t = \frac{1}{C}\int_0^L (T_w+bx)^{-1/2}dx$$

$$= \frac{2}{Cb}(T_w+bx)\Big]_0^L$$

$$= \frac{2}{Cb}\left[(T_w+bL)^{1/2} - T_w^{1/2}\right]$$

From equation (10)

$$b = (T_\infty - T_w) / L$$

Substitute to equation (12), we have

$$t = \frac{2L}{T_\infty - T_w}(T_\infty^{1/2} - T_w^{1/2})$$

$$t = \frac{2L}{C}\left(\frac{1}{\sqrt{T_\infty} + \sqrt{T_w}}\right) \tag{13}$$

If no temperature gradient,

$$t = L/a = L/C\sqrt{T_{sv}} \tag{14}$$

Equating equations (13) to (14), we have

$$T_{sv} = \frac{1}{4}\left(\sqrt{T_\infty} + \sqrt{T_w}\right)^2 \tag{15}$$

The magnitude of this effect is believed to be small, but its evaluation in the engine experiments is difficult because of the unknown gas transport velocity pattern within the test chamber.

RESULTS AND DISCUSSIONS:

The effect of gage length on bar tip temperature was shown in figure 15. It can be seen that for any particular length of transducer bar tip, the tip temperature will be a function of engine conditions, in this case, it is the speed. It is also evident that the thermal conductivity of the bar will change the slope of the curves of figure 15, as can be seen in figure 22.

The effect of gage length on end gas temperature was shown in figure 16. The curves in figure 16 indicates that the transducer bar tips are probably cooling the gas when the gas is much hotter than bar as at top center, or vise versa, when the gas is cooler than the bars. From figure 16, it also appears that with a large enough gap, 1/2 inch or more, the boundary layer is thin enough so that influence of the wall is negligible.

It was experienced during the experiments that if the path is short, a more readable signal results, this is due to the fact that attenuation of the signal in the gas is reduced. With the small gap, the scatter of points is not appreciably worse than with the large gap as shown in figure 15. Also, it was possible to read signals at a much lower gas density - as early as 120 degrees before top center, as shown in figure 17-A. But, on other hand, the time for the sound pulse to propagate the gap is reduced, the errors in time measurements are more significant. And a slight error committed in gage length measurement will give a greater error in sound

velocity (i.e., temperature) measurement for a small gap than the large one. With the large gap, the signals were too poor to read earlier than 60°BTC* or sometimes 40°BTC if the engine is firing at 2000 rpm.

From figures 17, 18, 19 and 20, the temperatures measured is 100 degrees at 30°BTC and 150°F at top center, respectively, lower with the small gap. This could probably be due to the cooling effect of the bars./

To determine the optimum length of gas path to be used is therefore a compromise between the signal readability and the accuracy of the time measurement, attenuation of signal, operating temperature of the transducer bar tip, and the resulting effect of thermal boundary layer on the interpretation of temperature measured from the sound measured. Therefore, we can set a design criteria for the transducer: a) The transducer rod tips must be sufficiently cooled. This requirement means that the bars should not project unnecessary far into the chamber, b) The length of the gas path used must be large enough so that transit time can be measured with sufficient accuracy.

Figure 22 shows the effect of varying transducer bar material on tip temperature. The bar has a fixed path, 0.23 inch and the engine conditions were maintained the same for both the brass bar and steel bar measurement. It was indicated in figure 22 that the steel bar gave a 540°F at 1000 rpm firing and 580°F at 2000 rpm firing, respectively, higher temperature than the brass bar. The steel bar gave a 130°F different at both 1000 rpm and 2000 rpm motoring respectively. The fact that the steel bar gave

---

* BTC - before top center

a higher tip temperature could be due to the lower thermal conductivity* it has compared with the brass. For a constant heat transfer, the temperature seems to vary inversely as the thermal conductivity of the material.

Figure 23 and 24 shows the effect of transducer bar material on the end gas temperature measured by the sound velocity method, both at engine firing and engine motoring, respectively. As was expected, it indicates that the steel bar gave a higher end gas temperature. The temperature difference was about 200 to 250°R at top center. This could possibly be due to the fact that sound travels faster in steel at elevated temperature than at room temperature, while the reverse is true for brass in the temperature ranges encounter in these experiments.

We have the general wave propagation equation,

$$\nabla^2 \phi = \frac{1}{a^2} \frac{\partial^2 \phi}{\partial t^2} \tag{16}$$

where $$\nabla^2 = \partial^2/\partial x^2 + \partial^2/\partial y^2 + \partial^2/\partial z^2 \tag{17}$$

ϕ is a function of the position coordinates (x,y,z)
t is the time
a is the velocity of the propagating wave

If we consider the longitudinal propagation only, then we have a one-dimensional wave equation,

$$\frac{\partial^2 \phi}{\partial x^2} = \frac{1}{a^2} \frac{\partial^2 \phi}{\partial t^2} \tag{18}$$

---

* Thermal conductivity for brass, k = 2.7 watts/in-°C
for steel, k = 1.16 watts/in-°C

Let us consider a solid deformed along its axis, x. Hooke's law then takes the form:

$$F_x = -AE \frac{du}{dx} \qquad (19)$$

where A is the cross section of the bar,
du/dx is the longitudinal strain,
E is the Young's modulus
u is a function of x.

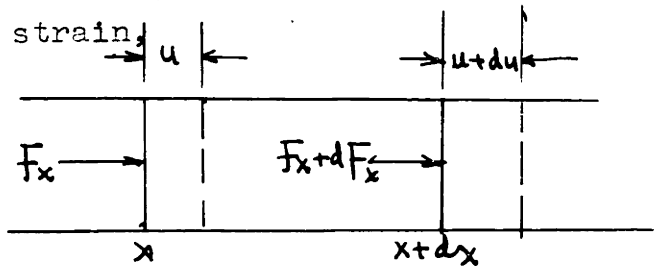

Figure 28

Let us take a section dx. The force at x is F_x and the force at x + dx is

$$F_x + dF_x = F_x + (\partial F_x/\partial x)\, dx \qquad (20)$$

With the use of equation (19) the net force will then be:

$$\frac{\partial F_x}{\partial x} dx = -AE \frac{\partial^2 u}{\partial x^2} dx \qquad (21)$$

This elastic force will be in dynamic equilibrium with the inetial reaction of the mass element $\rho A dx$:

$$-AE \frac{\partial^2 u}{\partial x^2} dx = \rho A \frac{\partial^2 u}{\partial t^2} dx \qquad (22)$$

where ρ is the density of the material.
which reduces to:

$$\frac{E}{\rho} \frac{\partial^2 u}{\partial x^2} + \frac{\partial^2 u}{\partial t^2} = 0 \qquad (23)$$

Comparing equation (23) with equation (18), we find for the extensional bar velocity, a_e :

$$a_e = \sqrt{E/\rho} \qquad (24)$$

Equation (24) holds true only for bar with lateral dimensions small compared with wavelength.

By considering wave transmission in a general medium by means of Christoffel's method and reducing the number of constants to correspond with isotropic symmetry, two types of wave can be propagated, namely, longitudinal waves in the direction of propagation and transverse or shear waves transverse to the direction of propagation. These two waves propagate with velocities:

$$a_L = \sqrt{(\lambda + 2\mu)/\rho}^{*} \qquad (25)$$

$$a_s = \sqrt{\mu/\rho} \qquad (26)$$

where a_L = longitudinal velocity
a_s = transverse velocity
λ = Lamé constant
μ = shear modulus
ρ = density

TABLE III-a**

Material	Yound's Modulus	Shear Modulus	Lamé Constant	PoissoN's ratio
Brass	10.4	3.8	11.3	0.374
Stainless Steel	19.6	7.57	11.3	0.300

TABLE III-b**

Material	Density	Longitudinal velocity	Shear Velocity	Extensional velocity
Brass	8.6	4,700	2,110	3,480
Stainless Steel	7.91	5,790	3,100	5,000

* Equations (25) and (26) has been derived in Ref. (26) Pages 368 - 73.

** Data used in Table III-a and Table III-b were taken from ref. (27).

Equation (24) holds true only for bar with lateral dimensions small compared with wavelength.

By considering wave transmission in a general medium by means of Christoffel's method and reducing the number of constants to correspond with isotropic symmetry, two types of wave can be propagated, namely, longitudinal waves in the direction of propagation and transverse or shear waves transverse to the direction of propagation. These two waves propagate with velocities:

$$a_L = \sqrt{(\lambda + 2\mu)/\rho} \quad (25)$$

$$a_s = \sqrt{\mu/\rho} \quad (26)$$

where a_L = longitudinal velocity
a_s = transverse velocity
λ = Lamé constant
μ = shear modulus
ρ = density

TABLE III-a**

Material	Yound's Modulus	Shear Modulus	Lamé Constant	PoissoN's ratio
Brass	10.4	3.8	11.3	0.374
Stainless Steel	19.6	7.57	11.3	0.300

TABLE III-b**

Material	Density	Longitudinal velocity	Shear Velocity	Extensional velocity
Brass	8.6	4,700	2,110	3,480
Stainless Steel	7.91	5,790	3,100	5,000

* Equations (25) and (26) has been derived in Ref. (26) Pages 368-373.

** Data used in Table III-a and Table III-b were taken from ref. (27).

Units used in Table III-a and Table III-b:

Young modulus, E - Newtons/m^2 x 10^{-10}
Shear modulus, μ - Newtons/m^2 x 10^{-10}
Lamé constant, λ - Newtons/m^2 x 10^{-10}
Longitudinal velocity, a_L - m/sec
Shear velocity, a_s - m/sec
Extensional velocity, a_e - m/sec
Density, ρ - g/cm^3

Table III show the different velocities for brass and steel. As shown, the sound velocity propagation is faster in steel than in brass.

The density for steel decreases as the temperature increase while the density for brass doesn't vary as much as the steel at elevated temperature (Ref. 29). The Lamé constant and shear modulus doesn't vary too much at elevated temperature. Therefore, the sound velocity at elevated temperature travel faster in the steel bar than the brass bar as can be seen in equation (25). The difference of sound velocity between calibration (room) temperature and test (elevated) temperature has been worked out experimentally. (Ref. 28).

The difference for bar-transit-time shift between calibration and operation may be corrected by trying to solve the total delay shift of a damped pressure wave train's time to pass thru a given bar by integrating the delay shift per inch of the bar held at some temperature t above the calibration temperature. (Ref. 28).

The General Electric Company have a project on this and the results yielded a + 0.084 micro-seconds total delay shift for the brass bars and a -0.25 micro-seconds for the steel bars. Thus, if we add a 0.25 micro-seconds to the total operating pulse-delay time in the steel bar, and subtract 0.084 micro-seconds in brass bar to correct

for the bar-transit-time shift between calibration and operation. This was done on the runs and the results gave a difference of 80-120°R still, instead of 200-250°R at top center.

The large temperature difference obtained from sound velocity measurement using brass bar and steel bar could be due to the heat transfer between the gas and the bar. As shown in figure 22, the steel bar gave a much higher tip temperature, it is hotter than the gas even before combustion. It is possible that the bar is heating the gas and the reverse is true for the brass bar. It is believe that using a 1/2 inch or larger gap, a smaller temperature difference might result as shown in figure 16, the end gas temperature at 1/2 inch or larger gap seems to be less affected by the bar tip temperature. But, still there will be a temperature difference caused by the difference in density and thermal conductivity of the material used. The only way to correct the difference is to correct the bar-transit-time shift in the bar between calibration and operation.

An analysis indicates that the selection of the best bar material from the point of minimizing bar-transit-time shift would be obtained by plotting the reciprocal of the product of the thermal conductivity of the bar metal and the difference between the sound velocity of the bar metal at some elevated temperature and that of room temperature versus elevated temperature.

Figures 19, 20 and 23 shows that the curves seems to terminate a little sooner (flame arrival) in the open chamber used. This is due either to the fact that the spark plug location did not quite place the end-gas in the measuring zone, or to the longer flame travel required with the pocketed chamber, (Ref. 4), or both..

REMARKS:

A 1/2 inch gap should be tested with different material to give a clearer picture as to the effect of bar material in temperature measurement since 1/2 inch gap is less affected by tip temperature. The work of this thesis uses a 1/4 inch gap instead of a 1/2 inch gap as originally planned due to the mistake made in the fabrication of the transducer bar. But even with the 1/4 inch gap, the effect of the bar material on temperature measurement can be seen.

CONCLUSIONS

The sound velocity method can be used for measuring the gas temperature in a spark ignition engine if we choose the correct gap length and the right transducer bar material.

The gap length in the sound velocity method is an important factor to be consider. Increase in gap length is conducive to attenuation beyond the practical limits of the detection and amplification devices available, while reduction in gap length results in an increase in "wall effects" on the gas temperature. Also reduction in transit time for short gap increases the relative importance of the absolute errors present in the time measuring device. Hence we can determine the proper length of the gap that would be installed and operated in such a manner as to produce a minimum of interference with the temperature that a gage length of 1/2 inch to 5/8 inch would seem to be the ideal one.

We could also determine the best bar material to be used by plotting the reciprocal of the product of the thermal conductivity of the bar metal and the difference between the sound velocity of the bar metal at some elevated temperature and that of room temperature versus elevated temperature.

With correct gap length and bar material, the sound velocity method can give fairly accurate temperature measurement at high temperature and pressure, even at low temperature and pressure.

With the availability of sound velocity method for temperature measurement, we can analysis the engine cycle, it can be used in engine heat transfer studies and for construction of a fuel-air cycle. It can be used for polytropic exponent determination, estimation of residual gas present in an engine, study of knock etc... .

APPENDIX I

OBTAINING THE WORKING CURVE OF SOUND VELOCITY VS. TEMPERATURE

The end gas in an spark ignition engine is composed of air, fuel and residual gases. Since there is no published data on the exact thermodynamics properties of such mixtures at different temperatures, it is necessary to make certain assumptions about the mixtures. The important assumption made is that the end gas ia a mixture of perfect gases. For most of the constituents of the end gas, this is certainly a good assumption. The main portion consists of nitrogen and oxygen. They have very low critical temperatures and rather high critical pressures so that in the range encountered in an engine, a perfect gas assumption holds quite well. The most possible constituents to deviate from a perfect gas is the fuel in the mixture. But, the fuel-air ratio used in the engine is usually low (around or less than 0.08), the partial pressure of which is a very small fraction of the total pressure. Thus, in an engine, the fuel vapor pressure is a very small fraction of its critical pressure.

The range of temperature and pressure of an end gas is about 600 to 2000°R and 1 to 50 atms (total pressure). The following is a list of the critical values of some of the components of the end gas (Ref. 14). A generalized μ chart from the same reference shows how well the perfect-gas law holds at low pressures and high temperatures with respect to the critical values.

	T (critical)	P(critical)
Oxygen	278°R	50 atm
Nitrogen	227°R	35.5 atm
CO_2	548°R	73 atm
N-heptane	972°R	27 atm

With the mixture considered as one of the perfect gases, its thermodynamic properties at various temperature can be calculated from the data on each constituent with the laws governing perfect gas mixtures. Data on these constituents are available in published data.

In order to obtain the curves of sound velocity vs temperature, the following steps were carried out:

1) For air, plot c vs T from data given in Keenan and Kaye: "Gas Tables", for air at low temperature.

2) For fuel-air mixture with no residuals:

   a) Find C_p for air and fuel (C_8H_{18} or C_7H_{16}) at various temperature (500 to 2000°R).

   b) $C_{p(mix)} = C_{p(air)} \cdot \frac{1}{1 + F} + C_{p(fuel)} \cdot \frac{F}{1 + F}$

   c) $M_{(mix)} = \frac{1 + F}{1/M_{air} + 1/M_{fuel}}$

   d) $R_{(mix)} = 1544/M_{(mix)}$

   e) $C_{v(mix)} = C_{p(mix)} - R_{(mix)}/J$

   f) $k_{(mix)} = C_{p(mix)}/C_{v(mix)}$

   g) $c = \sqrt{k(1544/M)(32.2T)}$ (all refer to mixture)

Go through (a) to (g) at each temperature. The above equations follow the Gibbs-Dalton Law.

3) For product of combustion:

a) Find the composition of the product for the given fuel-air ratio from Taylor and Taylor "Internal Combustion Engines".

b) For various temperatures find C_p for each component from the published data.

c) $C_{p(prod)} = C_{p1}W_1 + C_{p2}W_2 + \cdots\cdots\cdots$

where W_1, W_2, ... are percentage by weight of the components

d) $M_{(prod)} = \dfrac{1}{(W_1/M_1) + (W_2/M_2) + \cdots\cdots}$

e) $R_{(prod)} = 1544/M_{(prod)}$

f) $C_{v(prod)} = C_{p(prod)} - R_{(prod)}/J$

g) $k_{(prod)} = C_{p(prod)} / C_{v(prod)}$

h) $c = \sqrt{k(1544/M)(32.2)}$ for the product

Go through (a) to (h) for each temperature.

4) For mixture of air, fuel and residuals, go through steps outlined in (3), treating the mixture as composed of two perfect gases: the fresh fuel-air mixture and residual. Their percentage by weight in the mixture are 1-f and f respectively. f is the percent residuals.

The results of these calculations are shown in figures 12, 13-A, 13-B, and 14. These sets of sound velocity vs temperature curves were used in converting sound velocity data into temperature.

APPENDIX II

ESTIMATING AND MEASURING RESIDUAL PERCENTAGE

The amount of residuals as a percentage present in the cylinder could not be determined accurately for there was no way of determining the residual gas temperature. So, the residual percentage has been either arbitrarily assumed or estimated with the following theoretical method.

This method uses the theoretical fuel-air cycle calculations. First, a temperature for the residual is assumed. Calculate from this temperature, exhaust pressure, and clearance volume, the mass of residuals. Mix this with the fresh charge measured by the rotameter to obtain state 1 of the theoretical cycle. Go through a theoretical cycle calculation, using the Hottel charts. Arrive at state 5, which is the end of the expansion down to the exhaust pressure. The temperature at 5 may not agree with the assumed temperature. An iteration process is then used until the temperature at state 5 agress with the assumed residual temperature. This method does not take into acoount the effects of heat transfer, and it uses the theoretical cycle, which is different from the actual cycle. Therefore the result cannot be accurate. The residual percentage estimated by this method will be too low, as heat transfer will produce a denser residual gas.

Since the development of the sound velocity method, there is a tool to measure the gas temperature along the cycle. Thus it is no longer necessary to guess at the temperatures. The direct way to measure residual percentage would be: At some point on the expansion stroke before the exhaust valve opens, take a sound velocity

reading. Convert it into temperature, using the curve for products of combustion. From the temperature, the pressure from the indicator card, the cylinder volume corresponding to the crank angle, and the composition of the product of combustion, the total mass in the cylinder can be calculated with the perfect gas law. Subtracting the fresh charge per cycle from the total, the amount of residuals can be found.

The reading of sound velocity is sometimes difficult on the expansion stroke due to turbulence. Therefore a scheme using the temperature on the compression stroke is devised. First, assumed a residual percentage, Using the curve for fresh charge plus this percentage of residuals, obtain the temperature at a point on the compression stroke where the temperature is likely to be uniform throughout the cylinder. Calculate the total mass in the cylinder from the perfect gas law, using a gas constant computed for this particular mixture. The residual mass is again obtained by subtracting the fresh charge from the total. If this amount does not agree with the first assumption, use an iteration process until the assumed percentage is correct.

The percentage of residuals present in the cylinder can be calculated by the following equation:

$$f = 1 - \frac{M(1 + F)\,RT}{pVm}$$

where f - mass residual gas per mass charge
M - mass of air entering cylinder during one induction stroke
F - fuel-air ratio, by weight
R - universal gas constant
T - absolute temperature

p - absolute pressure
V - volume
m - molecular weight

The accuracy of this method of calculation of residuals depends not only on the accuracy of measurement of p, V, M and T, but on the assumption average temperature in the cylinder. As can be seen from the equation above, if the measured temperature is lower than the average temperature, the value obtained for the percentage of residuals is greater than the correct value.

REFERENCES AND BIBLIOGRAPHY

1. Anon, "Four Proposed Methods of Measuring End Gas Properties", CRC Inc., 1953

2. Taylor, C.F., Livengood, J.C., etc. "Final Report on Development of Method for Measuring Gas Temperature of an Internal Combustion Engine" 1953-1954

3. Wu, P.C., "Engine End Gas Temperature Measurement and Detonation Study by the Sound Velocity Method", M.I.T., M.E. Thesis, 1953

4. Livengood, J.C., Taylor, C.F., and Wu, P.C., "Measurement of Gas temperature in an Engine by Velocity of Sound Method", SAE Transaction Volume 66, pages 638-699, 1958

5. Hirogoyen, B.C.J., "Study of End Gas Temperature in a Fuel Injection Spark Ignition Engine", M.I.T., M.E. Thesis, 1958

6. Livengood, J.C., "Method of Measuring the Velocity of Propagation of Sound in the Unburned Gas in an Otto Cycle Engine", M.I.T., Sloan Laboratory Report, 1952

7. Ronn, T.P., "Measurement of Ultrasonic Propagation Velocity of Gases", M.I.T.,.E.E. Thesis, 1953.

8. Ronn, T.P., "Gas Temperature Measurement by Ultrasonic Pulse Method", M.I.T., E.E. Sc.D. Thesis, 1955

9. Leasry, W.A., and Tsai, D.H., "Metering of Gases by Means of ASME Square-edged Orifice with Flange Taps", Notes, Sloan Laboratory, M.I.T., July, 1951

10. Notes on Pressure Indicators, M.I.T. Sloan Laboratory

11. Uyehara, O.A., Myers, P.S., Watson, K.M., and Wilson, L.A.,"Flame Temperature Measurements in Internal Combustion Engines" ASME Transaction, Vol. 68, Jan., 1946, pages 17-30

12. ASME Transaction, 1947, page 465

13. Chen, K.S., "The Application for Absorption Spectra for Compression Temperature Measurements", Ph.D. Thesis

14. Keenan, J.H., "Thermodynamics", John Wiley and Sons., Inc., N.Y. 1936

15. Keenan, J.H., and Keyes, F.G., "Steam Tables", John Wiley and Sons, Inc., N.Y., 1936

16. Taylor, C.F. and Taylor, E.S., "The Internal Combustion Engine", International Textbook Co., 1948

17. Baruch, JJ., "Survey on Gas Temperature Measurement by Sound Velocity Method". MIT Sloan Lab., 1951

18. Angona, F.A., "Absorption of Sound in Gas Mixtures", JASA, Vol. 25, pages 1116-1122, 1953

19. Hueter, T.F., and Bolt, R.H., "Sonics" John Wiley and Sons, Inc., N.Y. 1954

20. Bourgin, D.G. "Sound Absorption and Velocity in Mixtures" Physical Review Vol. 50, pages 355-369, 1936

21. Mason, W.P.,"Electromechanical Transducer and Wave Filters", N.Y. Van Nostrand Co., Inc., 1949

22. Sints, C.G., "Determination of Arc Temperature from Sound Velocity Measurements", Physic. Review Vol. 6, page 190.

23. Zartman, I.F. "Measurement of Sound Velocity in Gases" JASA, Volume 21.

24. Hedrich, A.L., and Pardue, D.R., "Sound Velocity as A Measurement of Gas Temperature", Temperatures, Its Measurement and Control in Science and Industry, Volume 2, American Institute of Physics.

25. Notes on Propagation of Sound through a Gas with A Temperature Gradient, MIT Sloan Lab., Notes

26. Mason, W.P., "Physical Acoustics and the Properties of Solids", D. Van Nostrand Co., Inc., Princeton., N.J., 1958

27. American Institute of Physics Handbooks

28. Letter's Report on Measured Temperature Distribution Along the Acoustical Transducer Bars by Gene Oster of General Electric Comapny, Lynn, Mass.

29. American Society of Metals "Metal Handbook".

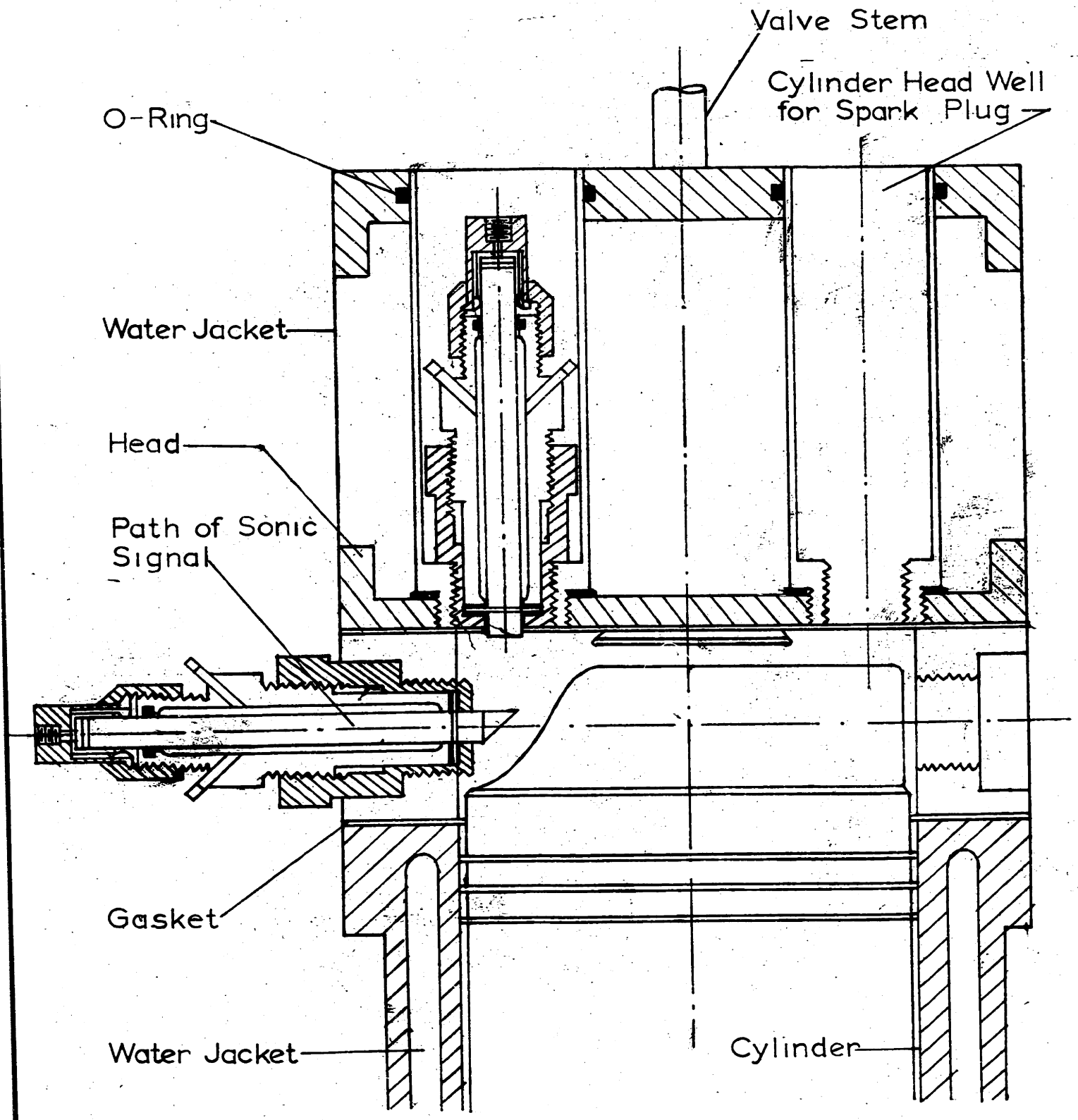

FIG. 1 SECTION SHOWING PATH OF SONIC SIGNAL IN FLAT CYLINDRICAL CHAMBER

ENGINE CONDITIONS:

1000 rpm Firing

CR = 6 F = 0.08

Fuel - Nat - Gas

S.A. 25° BTC

Pe - 3[illegible] lbs.

P - 28[illegible]

T - 100°F [illegible]°C

[illegible]

Three D[illegible]

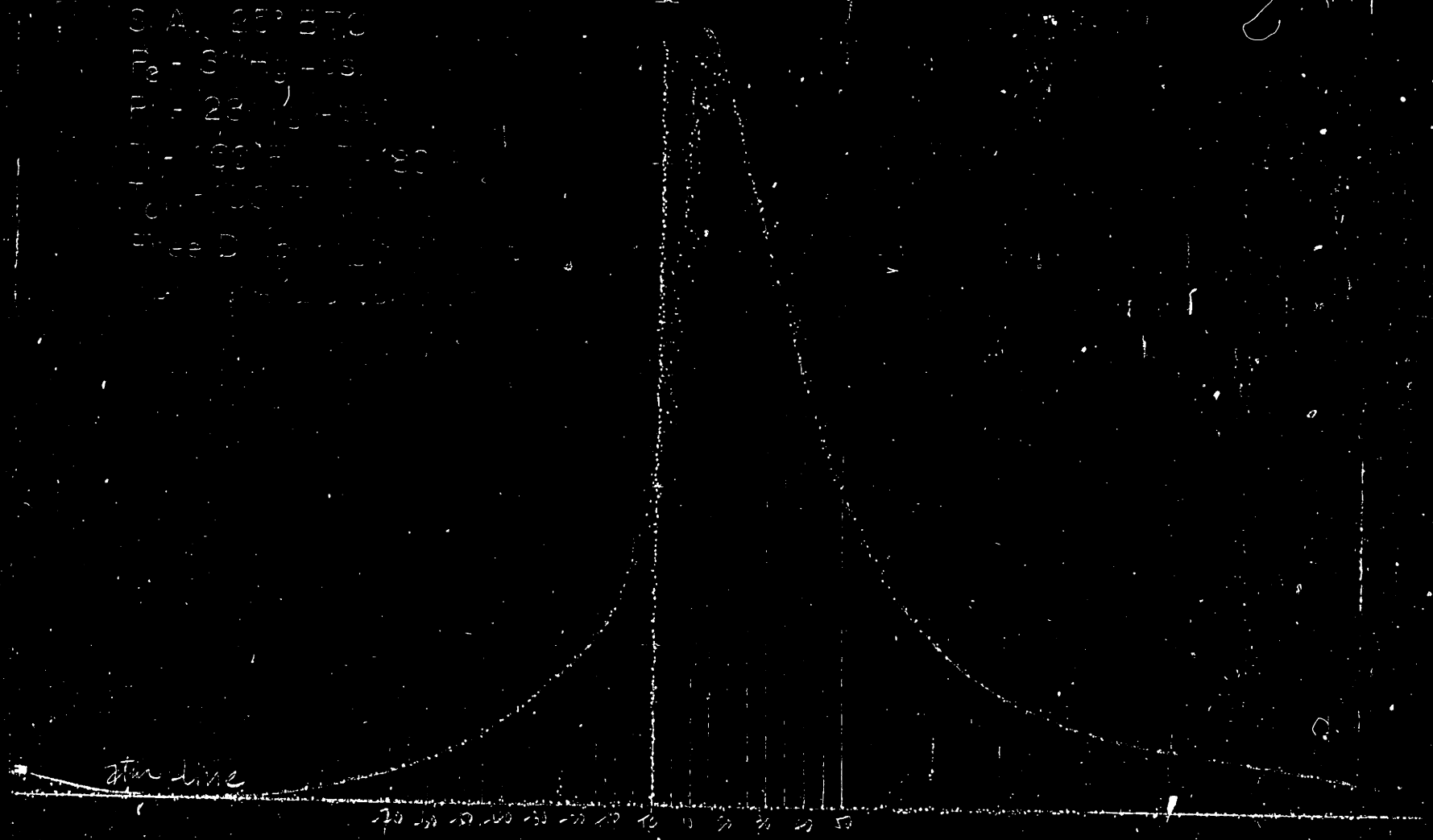

FIGURE 2 - INDICATOR CARD

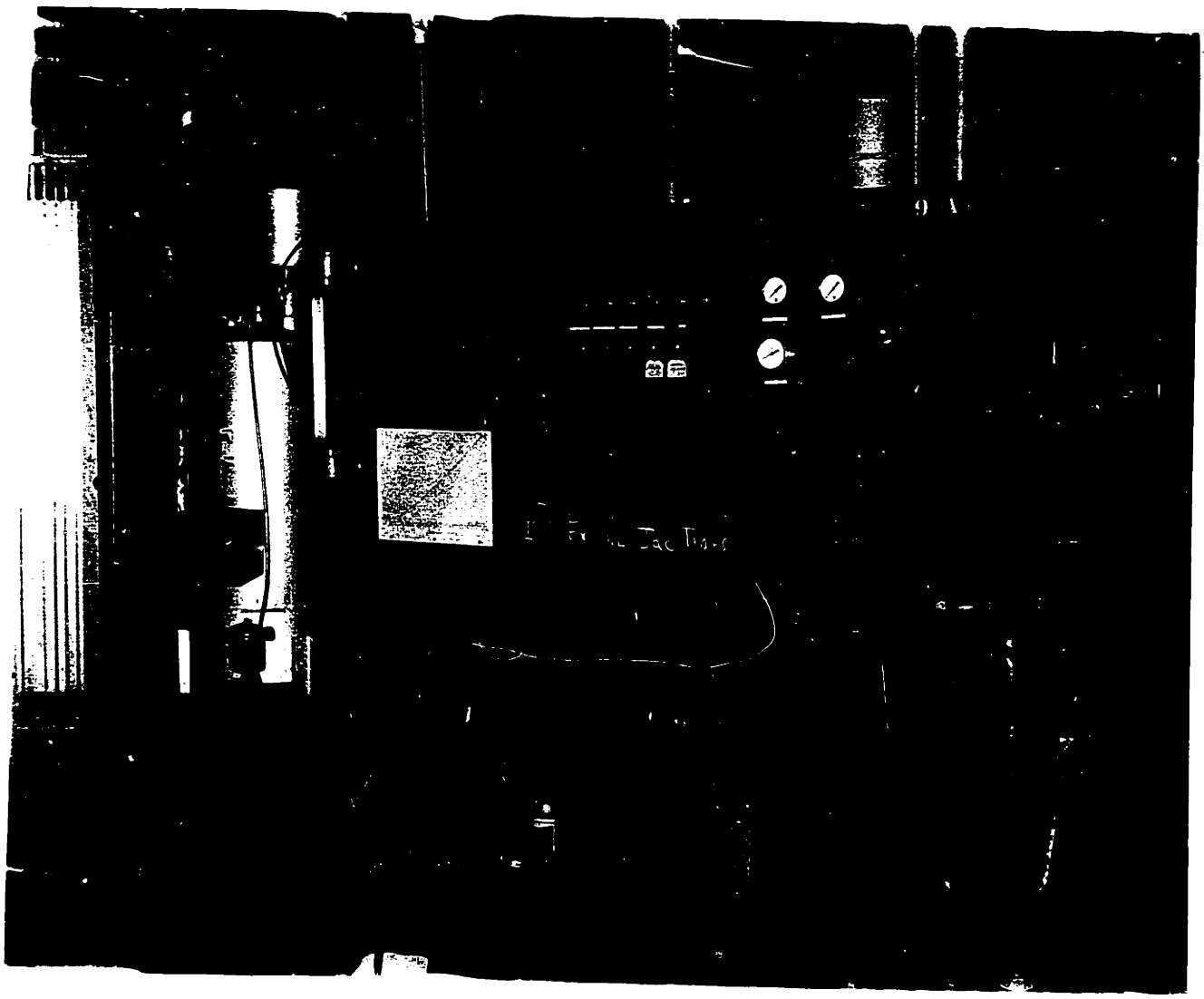

Figure 3 Front View of Sloan Automotive and Aircraft Laboratory Standard Engine set-up used for this thesis work.

Run No. 124 Date Jan 13 59

Engine 8V-71 Spring 100 psi/in.

C.R. 6, R.P.M. 1000, F 0.08

Fuel 80-octane Spark Advance 25 °BTC

p_e 31 "Hg Abs. p_i 28 "Hg Abs.

T_i 160 °F, T_j 180 °F, T_{oil} 150 °F

free diaphragm Pickup

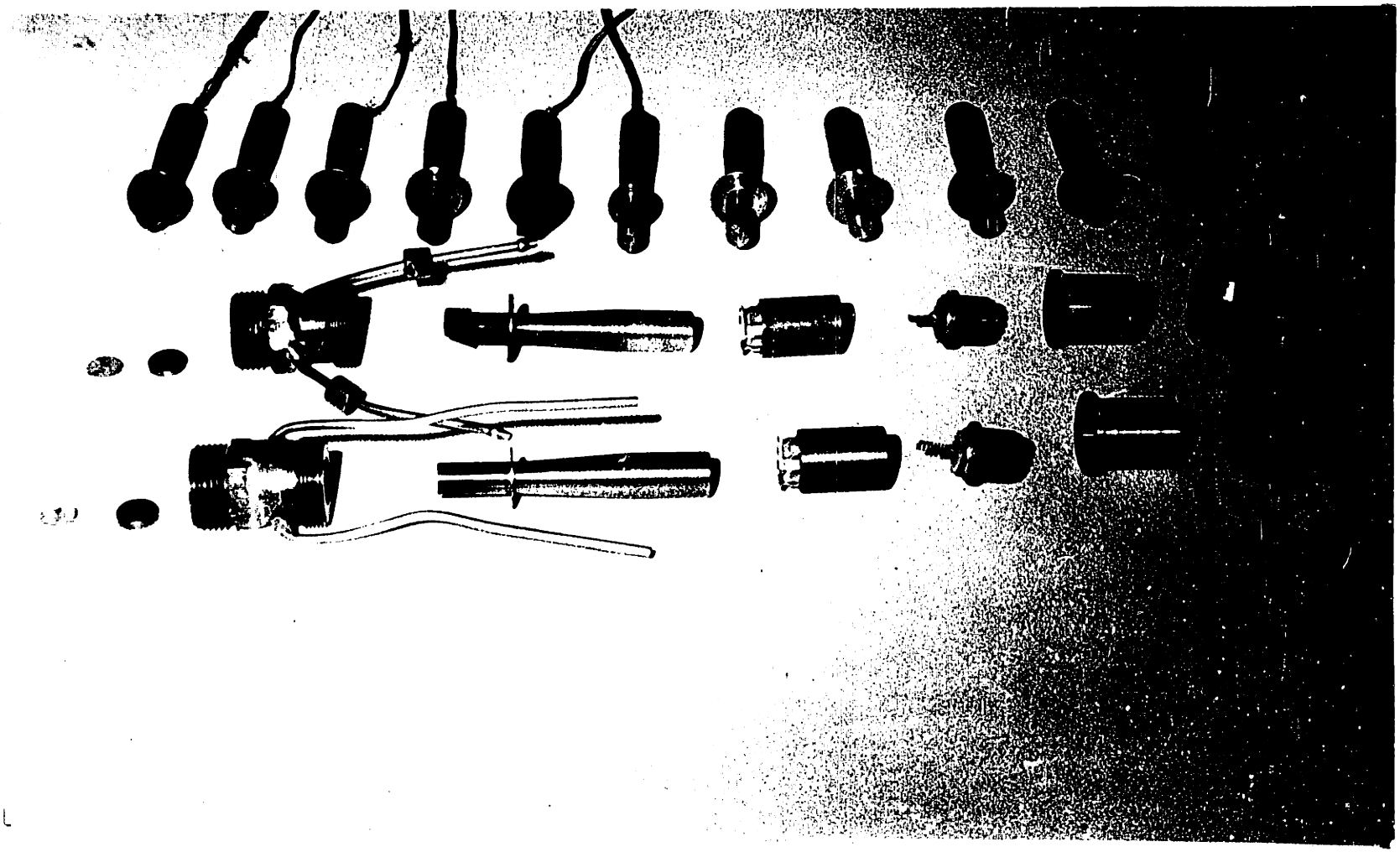

FIGURE 4 TRANSDUCER DETAILS & SIZES OF BARS USED

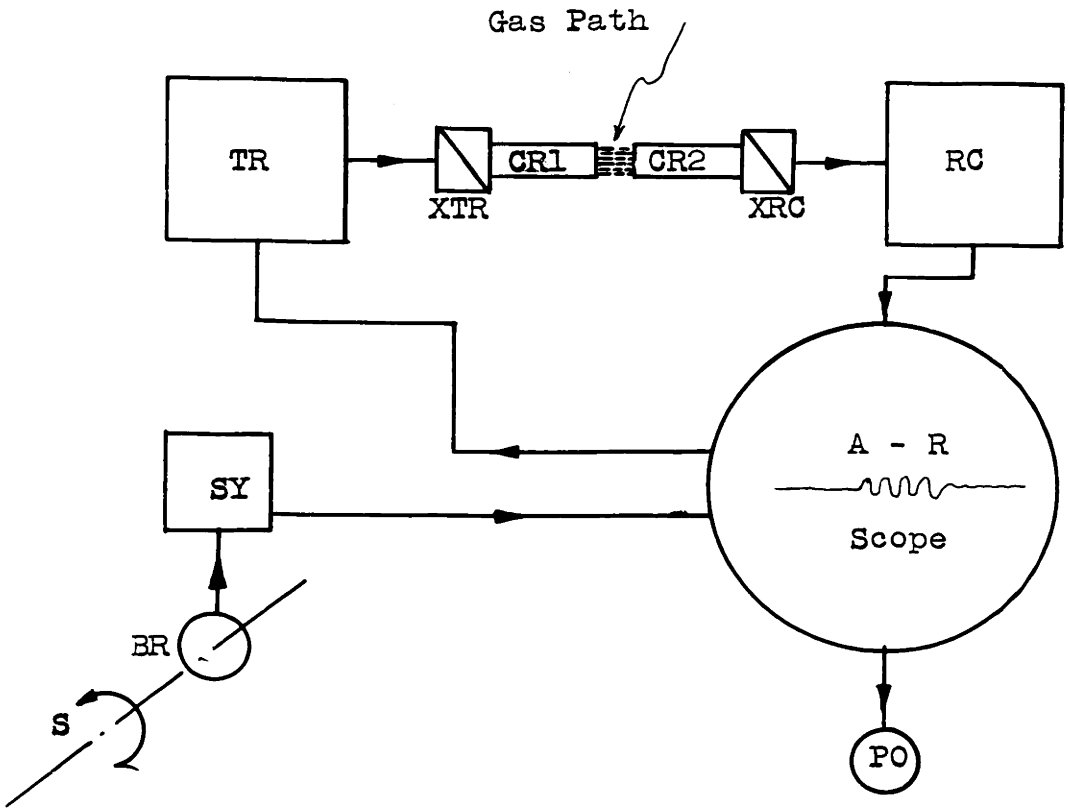

S	Engine Distribution Shaft
BR	Breaker
SY	Synchronizer
TR	Transmitter
XTR	Transmitter Crystal
XRC	Receiver Crystal
RC	Receiver
CR1	Coupling Rod 1
CR2	Coupling Rod 2
PO	Calibrated delay

Figure 5 Principle of the Apparatus Used

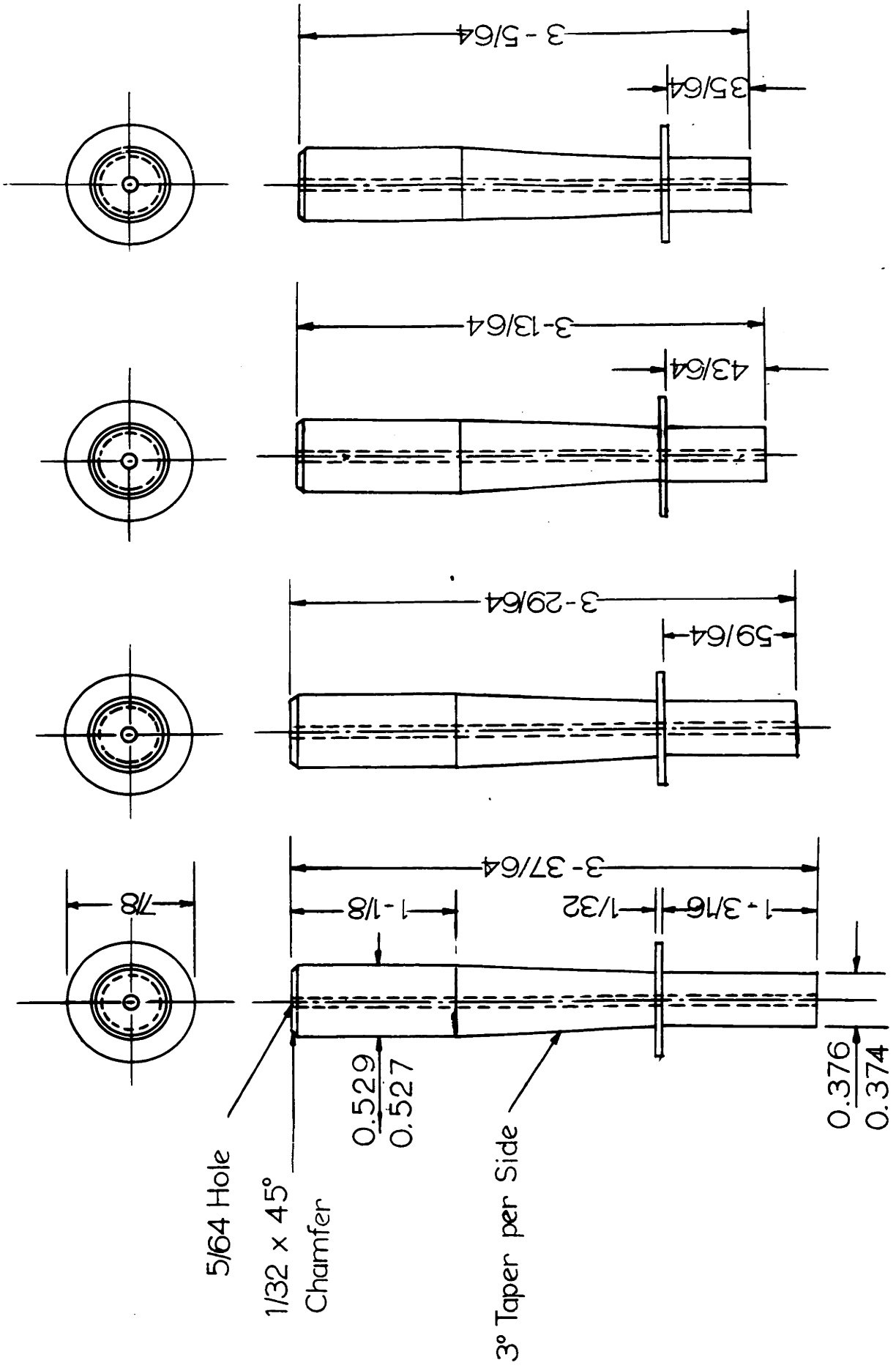

Figure 6 BRASS COUPLING ROD

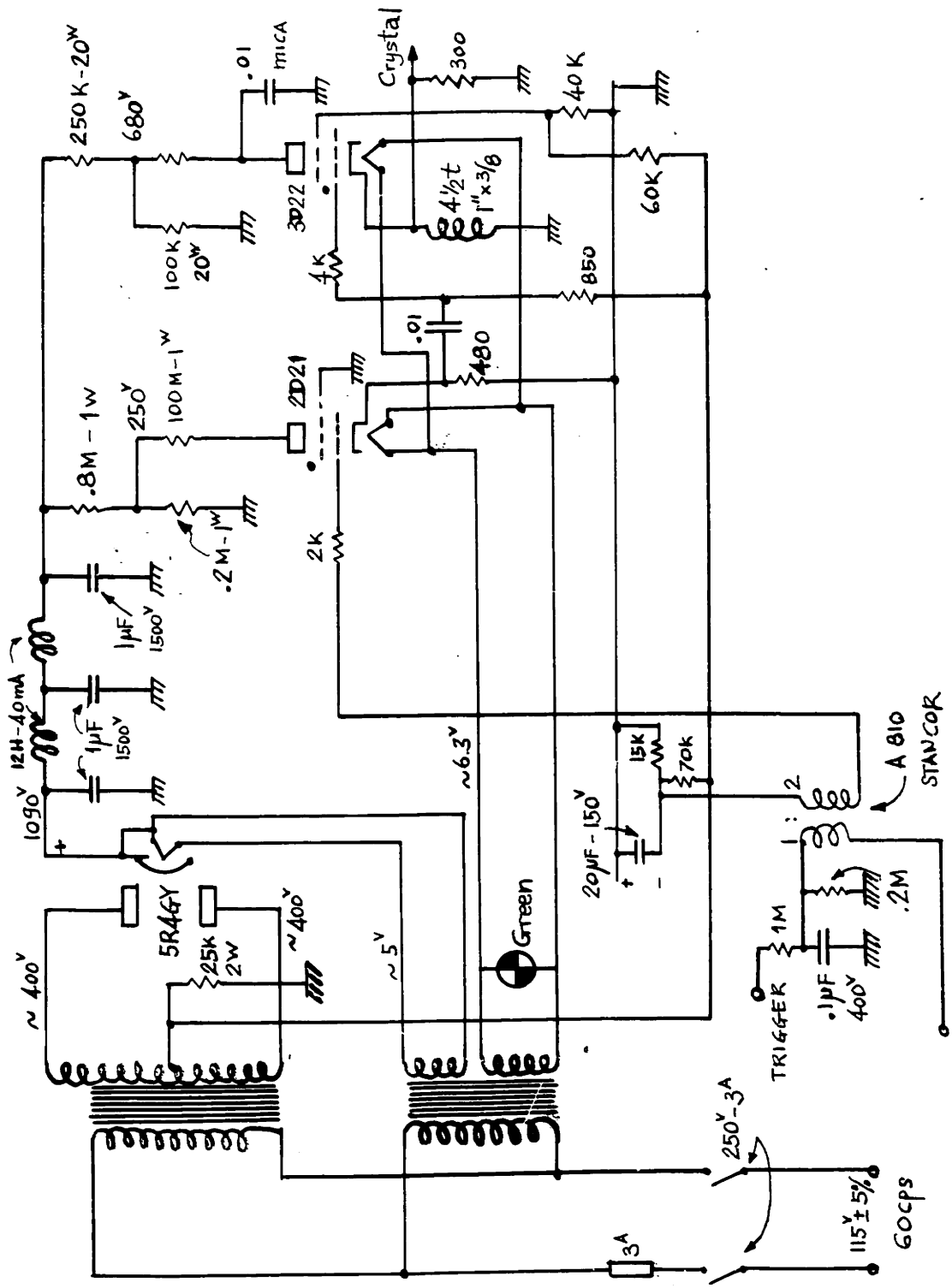

Figure 7 TRANSMITTER CIRCUIT

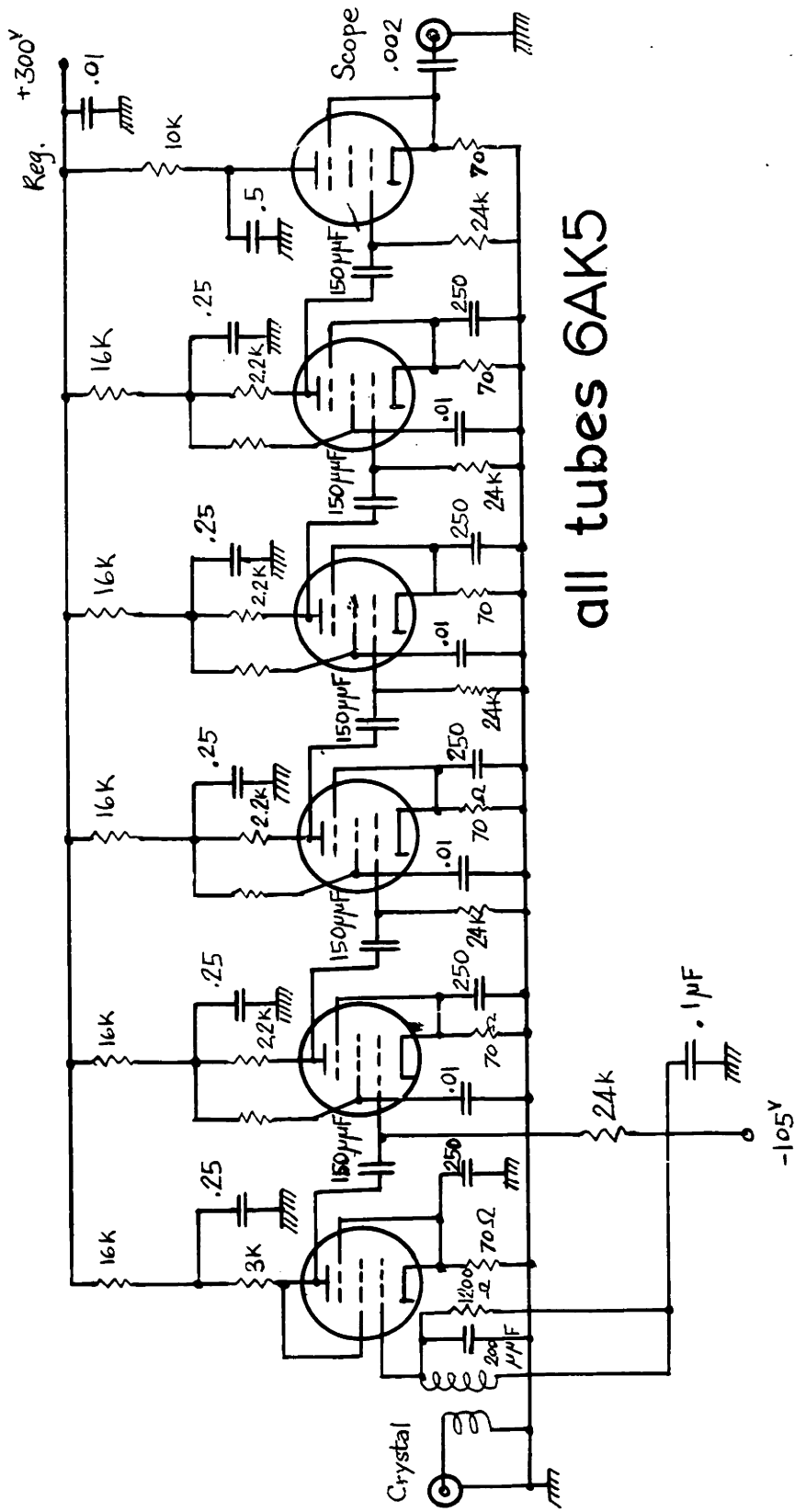

Figure 8 RECEIVER CIRCUIT

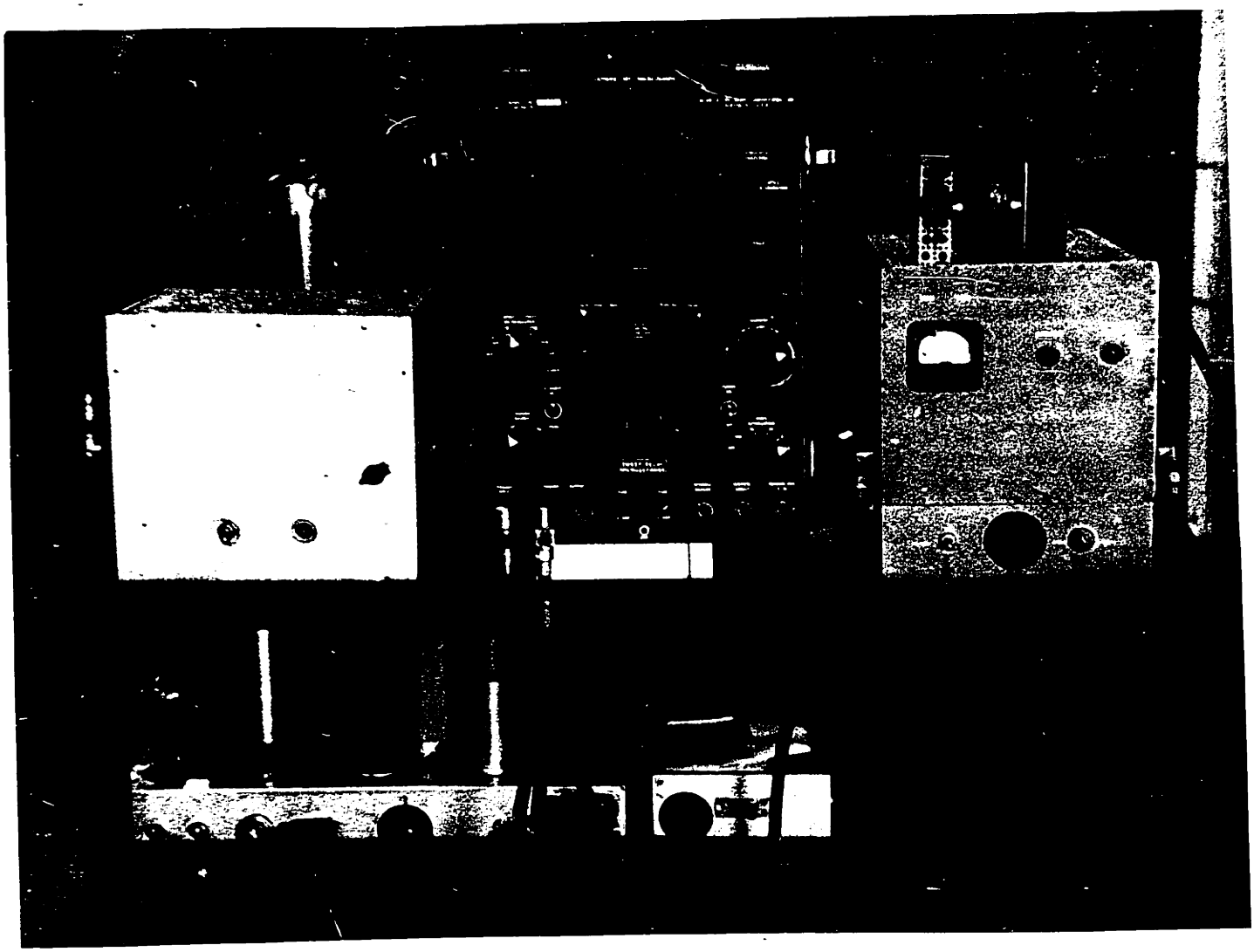

Figure 9 The Electronic Equipment

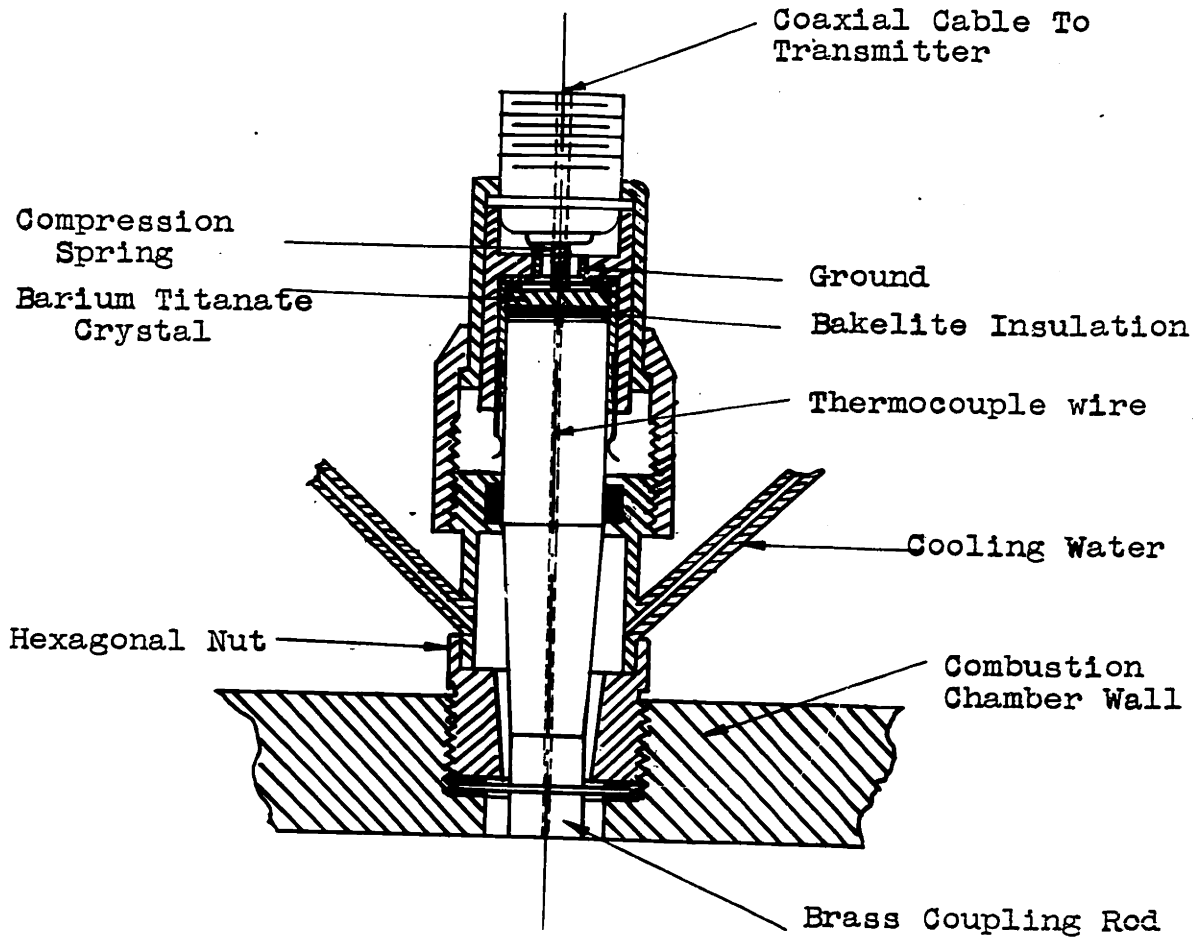

Figure 10 DETAILS OF TRANSDUCER

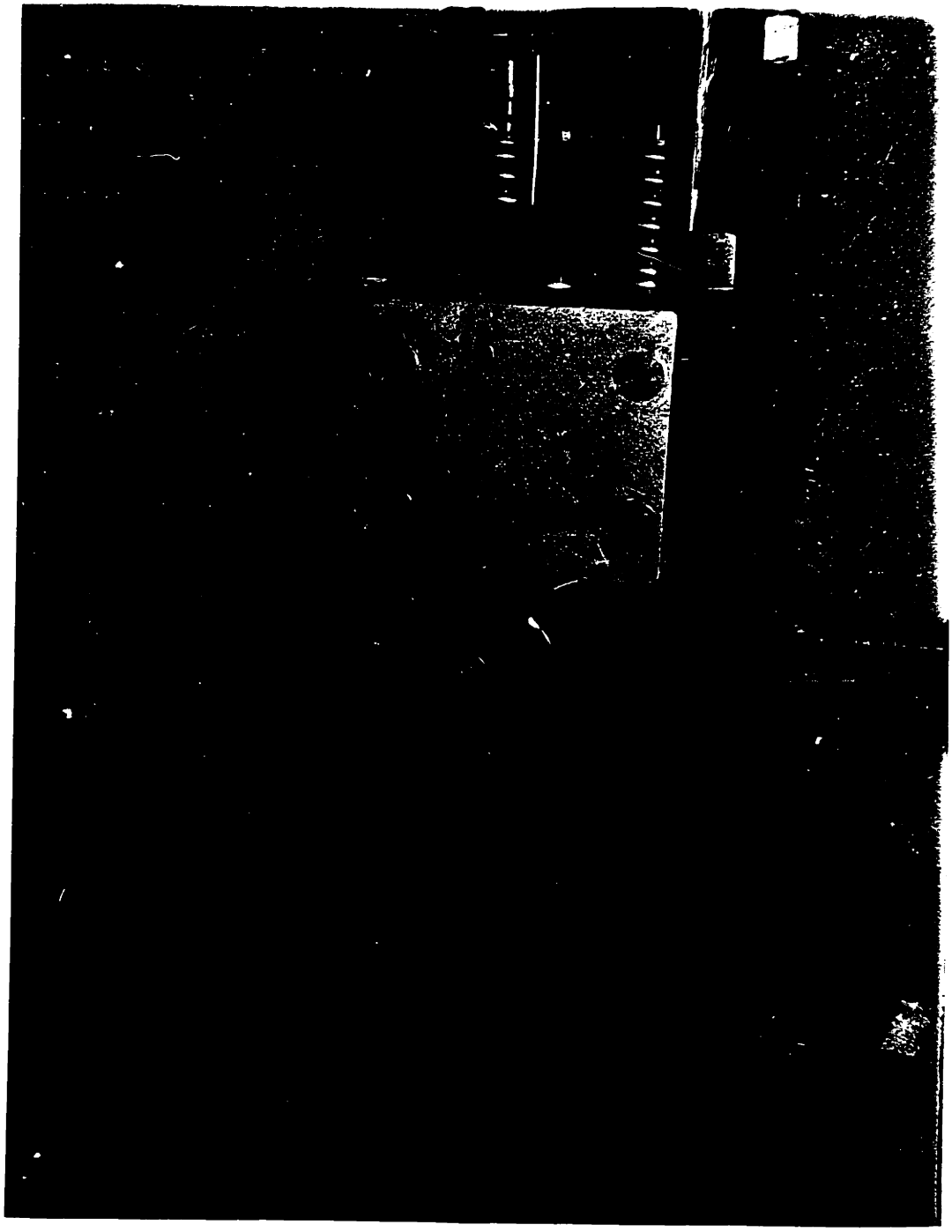

Figure 11 CFR single cylinder head with Transducer Mounted

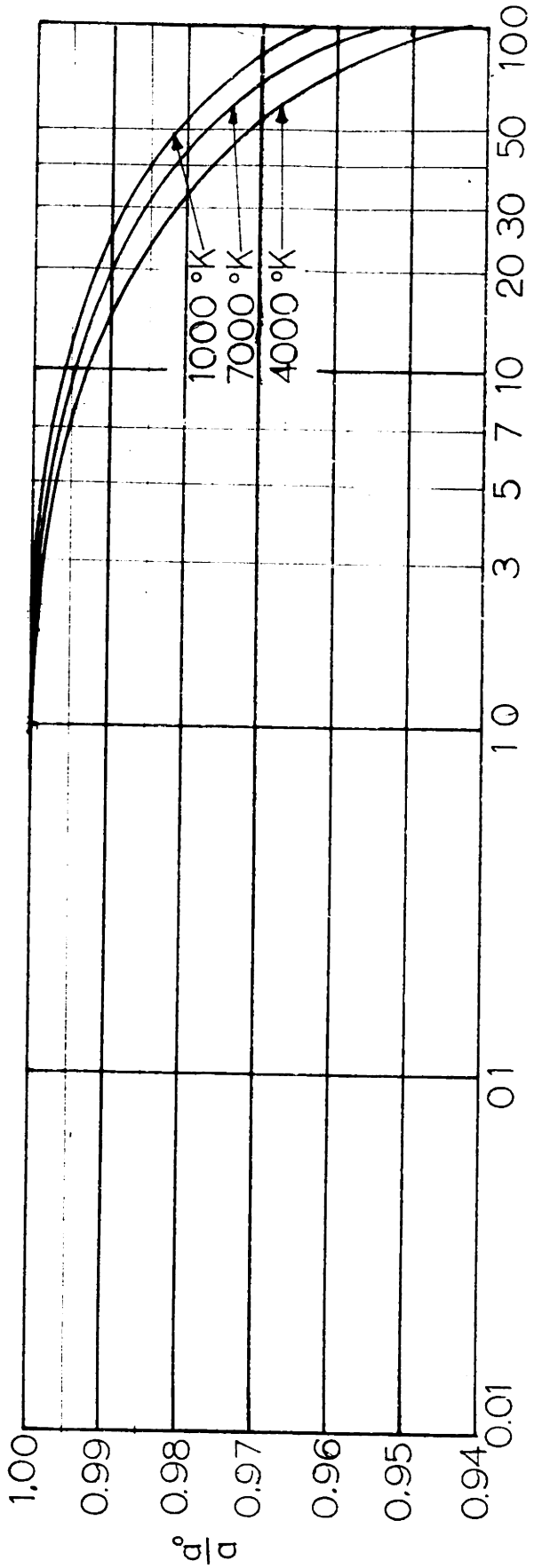

FIG. 12 PRESSURE EFFECT ON SOUND VELOCITY DRY AIR

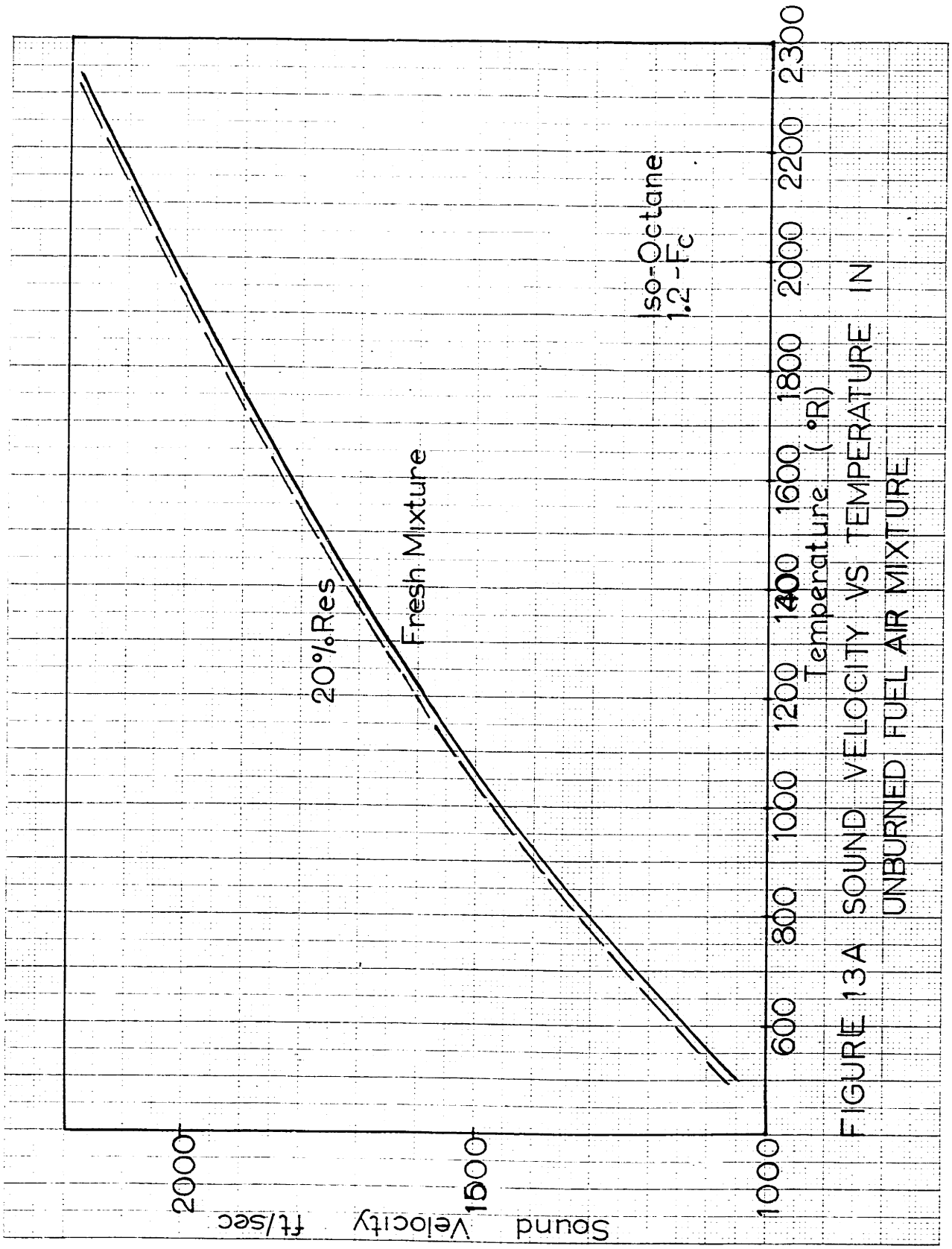

FIGURE 13A SOUND VELOCITY VS TEMPERATURE IN UNBURNED FUEL AIR MIXTURE

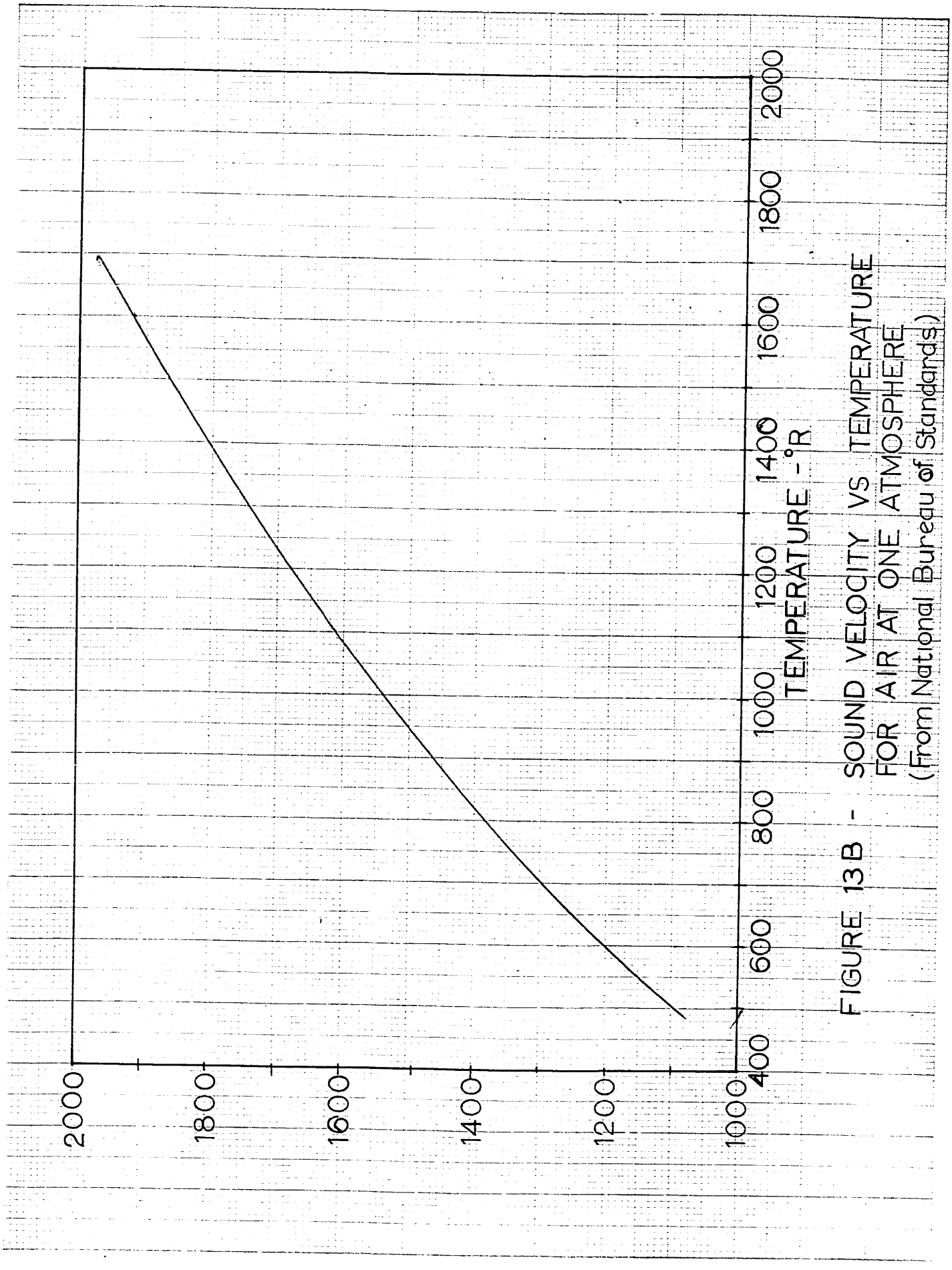

FIGURE 13B - SOUND VELOCITY VS TEMPERATURE FOR AIR AT ONE ATMOSPHERE (From National Bureau of Standards)

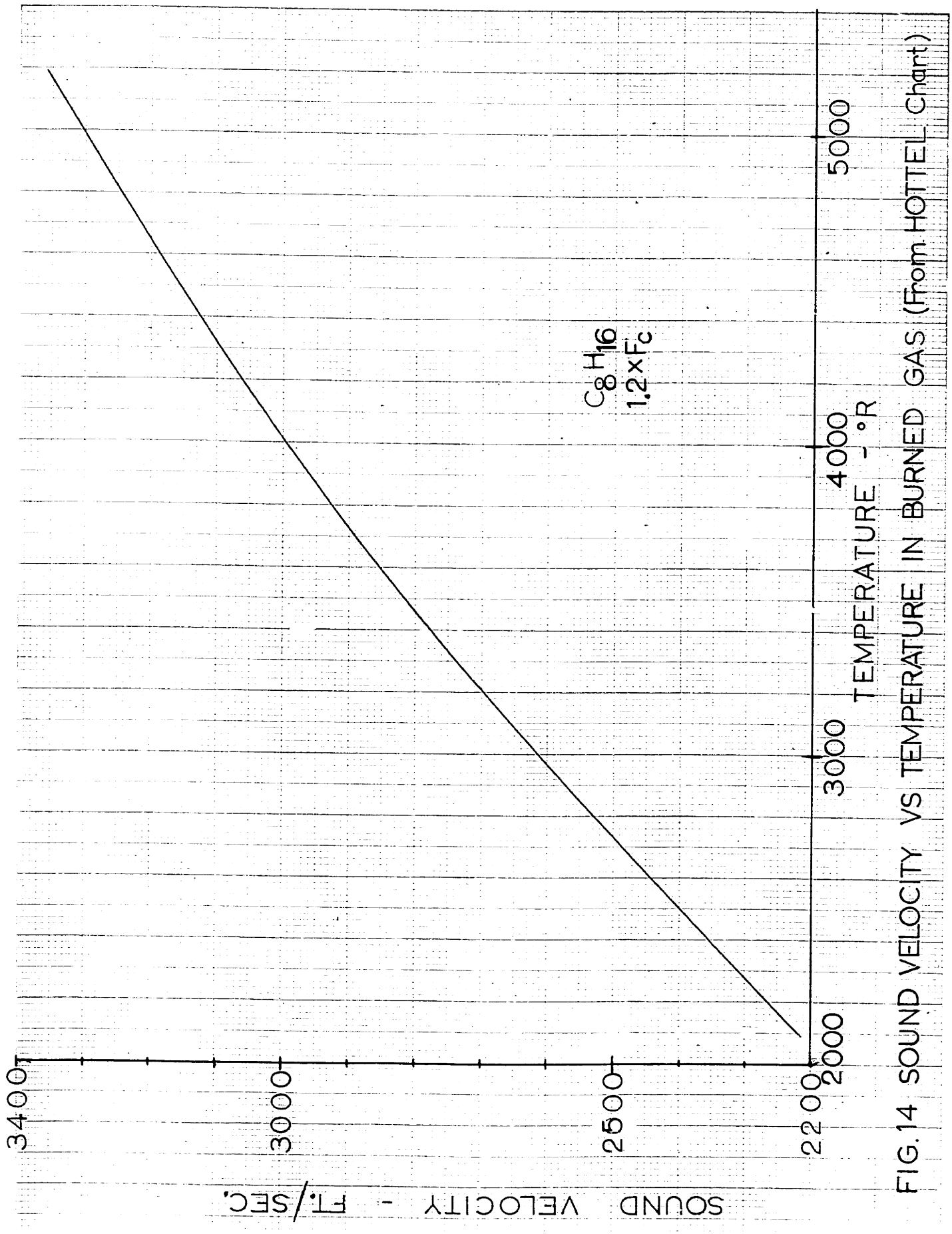

FIG. 14 SOUND VELOCITY VS TEMPERATURE IN BURNED GAS (From HOTTEL Chart)

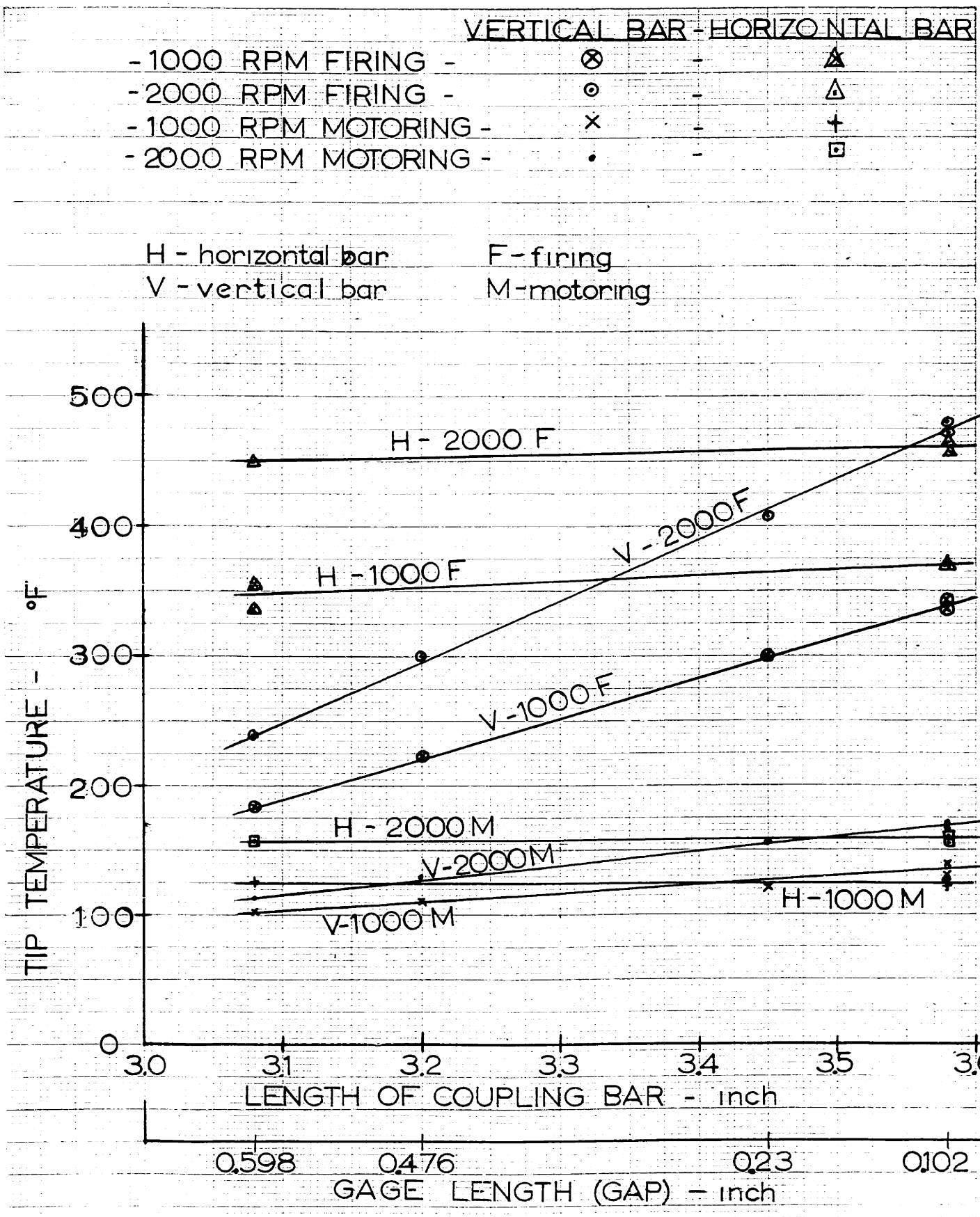

FIG. 15 EFFECT OF GAGE LENGTH ON TIP TEMPERATURE (BRASS BAR)

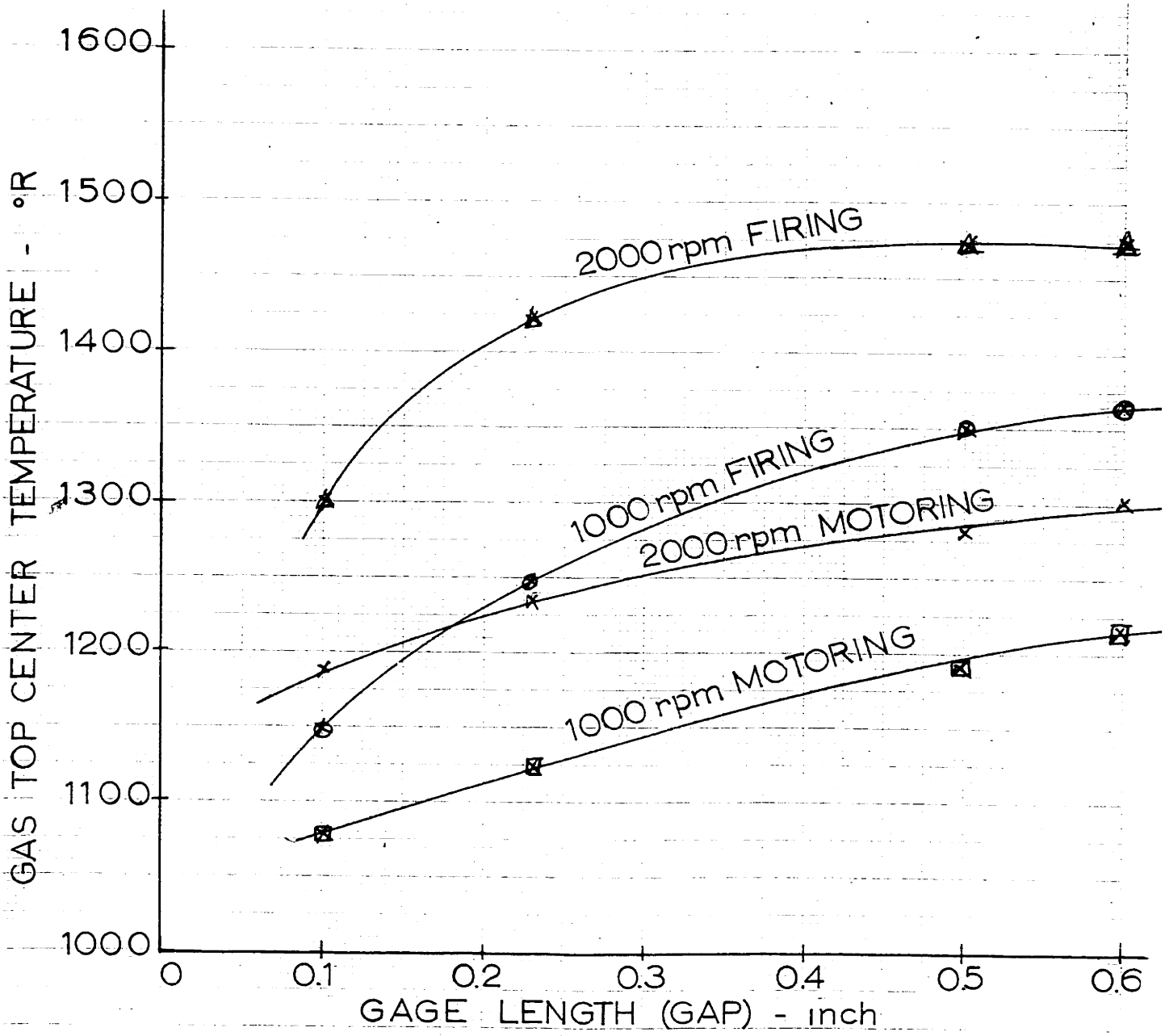

FIGURE 16 EFFECT OF GAGE LENGTH ON END GAS TEMPERATURE

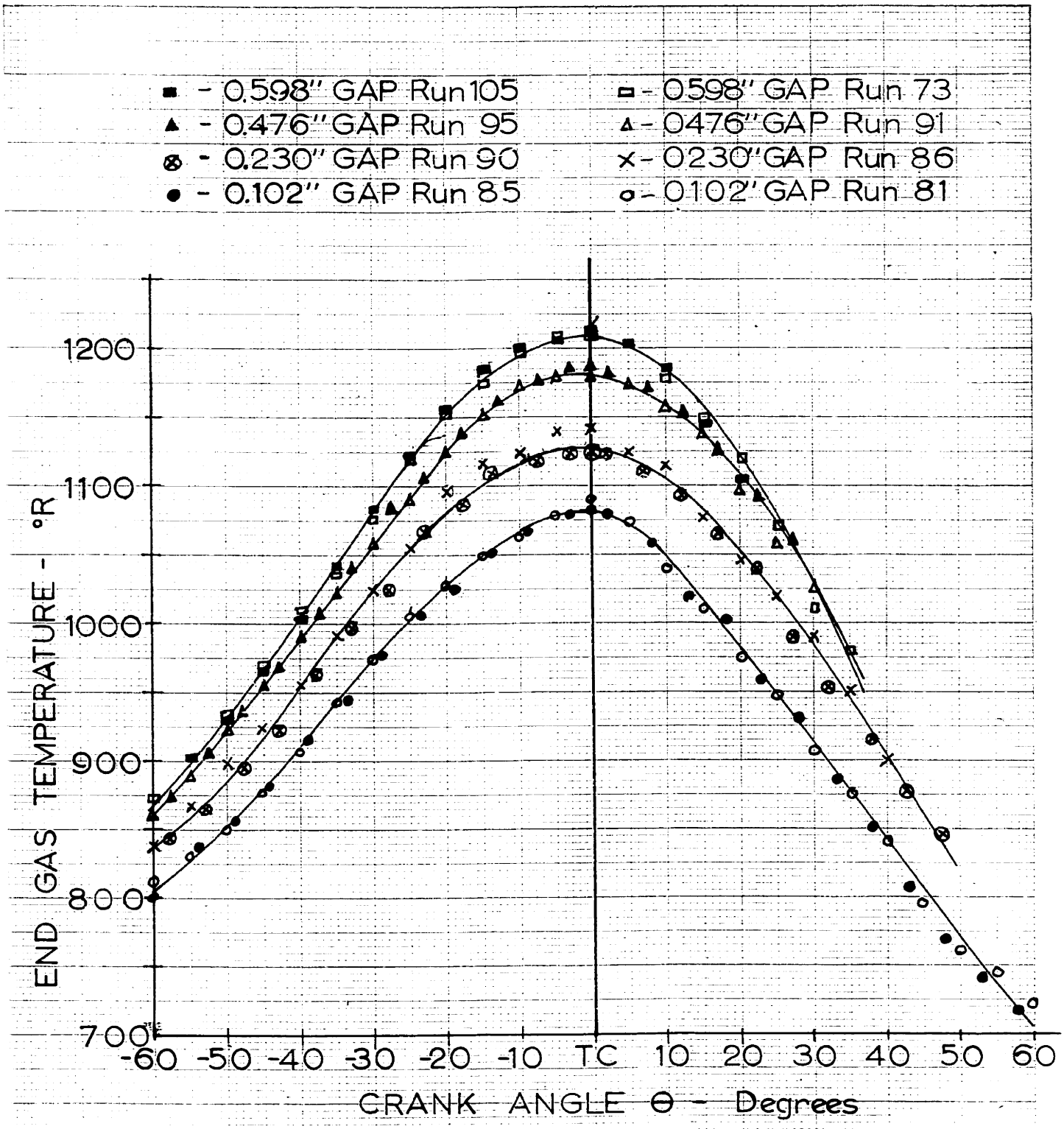

FIGURE 17 REPRODUCIBILITY AND EFFECT OF GAGE LENGTH ON END GAS TEMPERATURE AT 1000 RPM MOTORING USING BRASS BAR

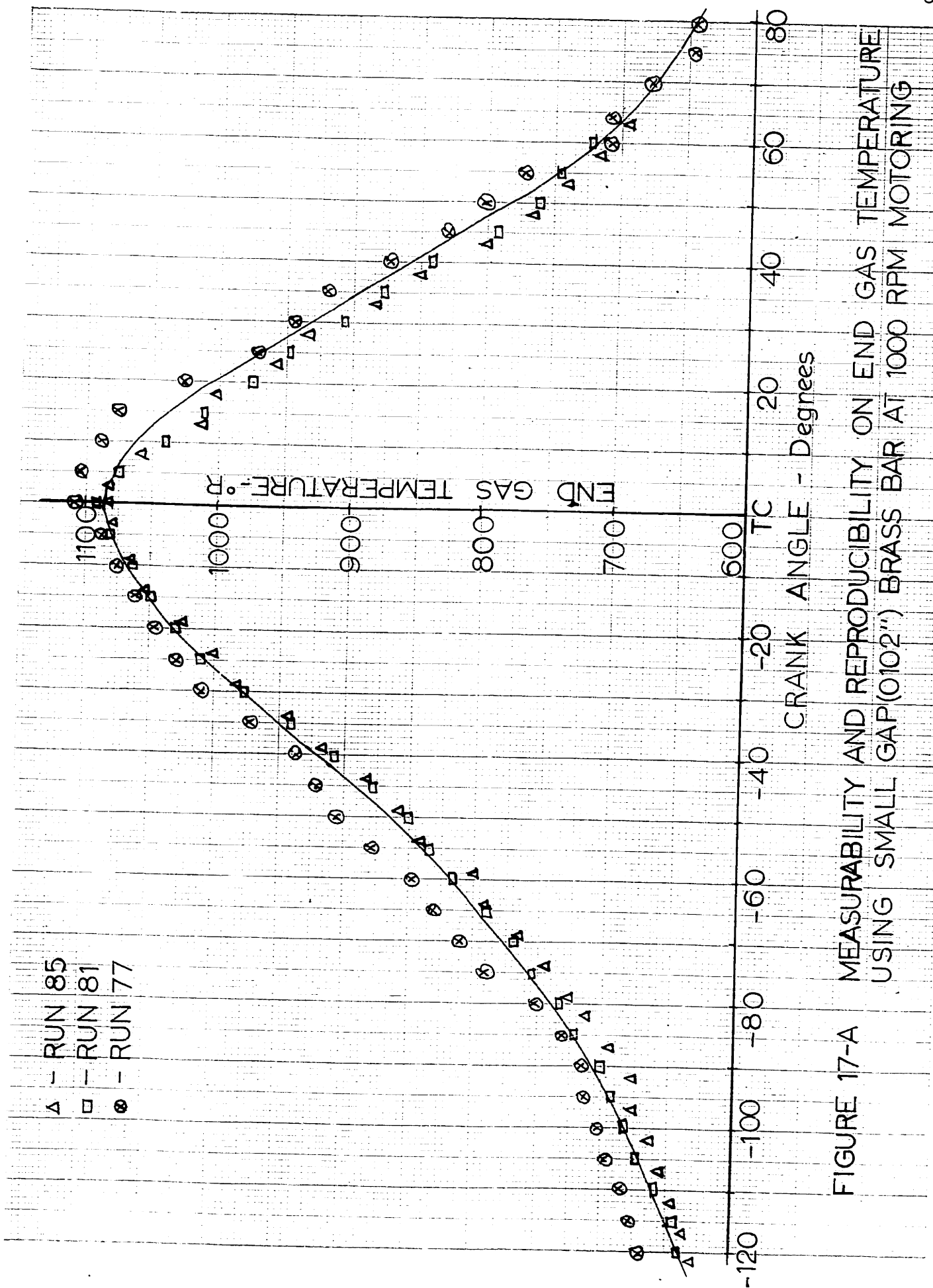

FIGURE 17-A MEASURABILITY AND REPRODUCIBILITY ON END GAS TEMPERATURE USING SMALL GAP(.0102") BRASS BAR AT 1000 RPM MOTORING

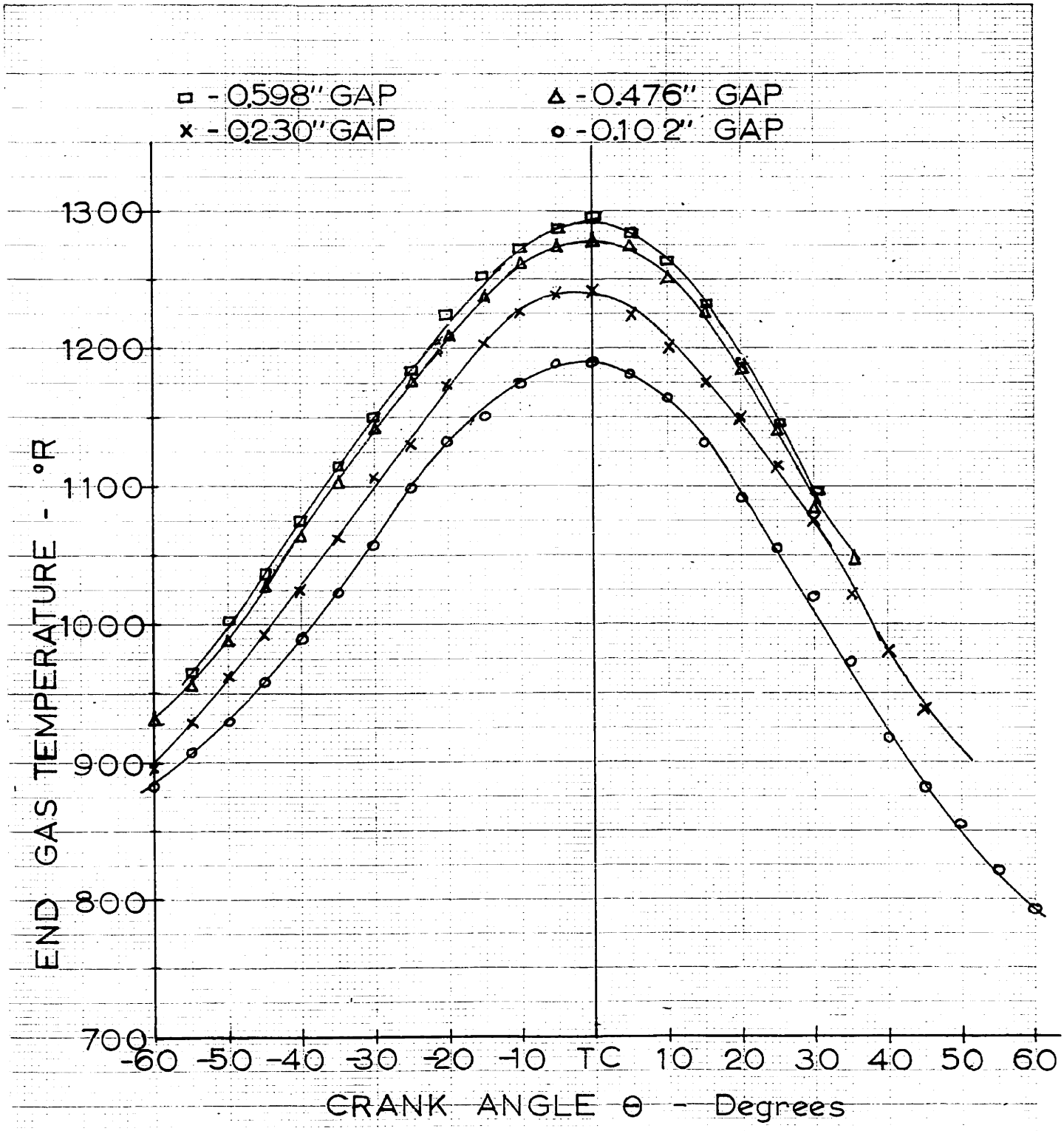

FIGURE 18 EFFECT OF GAGE LENGTH ON END GAS TEMPERATURE AT 2000 RPM MOTORING

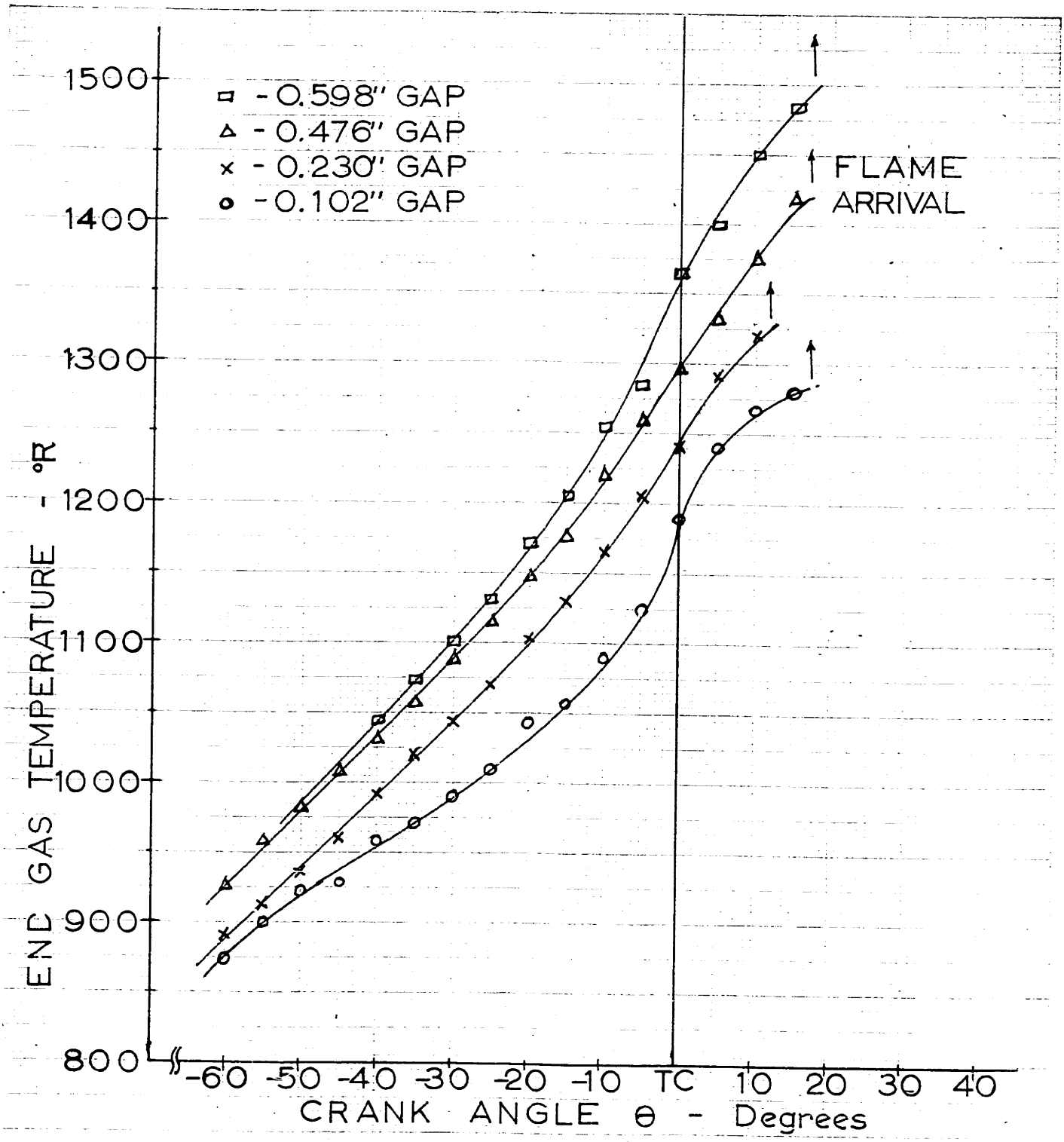

FIGURE 19 EFFECT OF GAGE LENGTH ON END GAS TEMPERATURE AT 1000 RPM FIRING

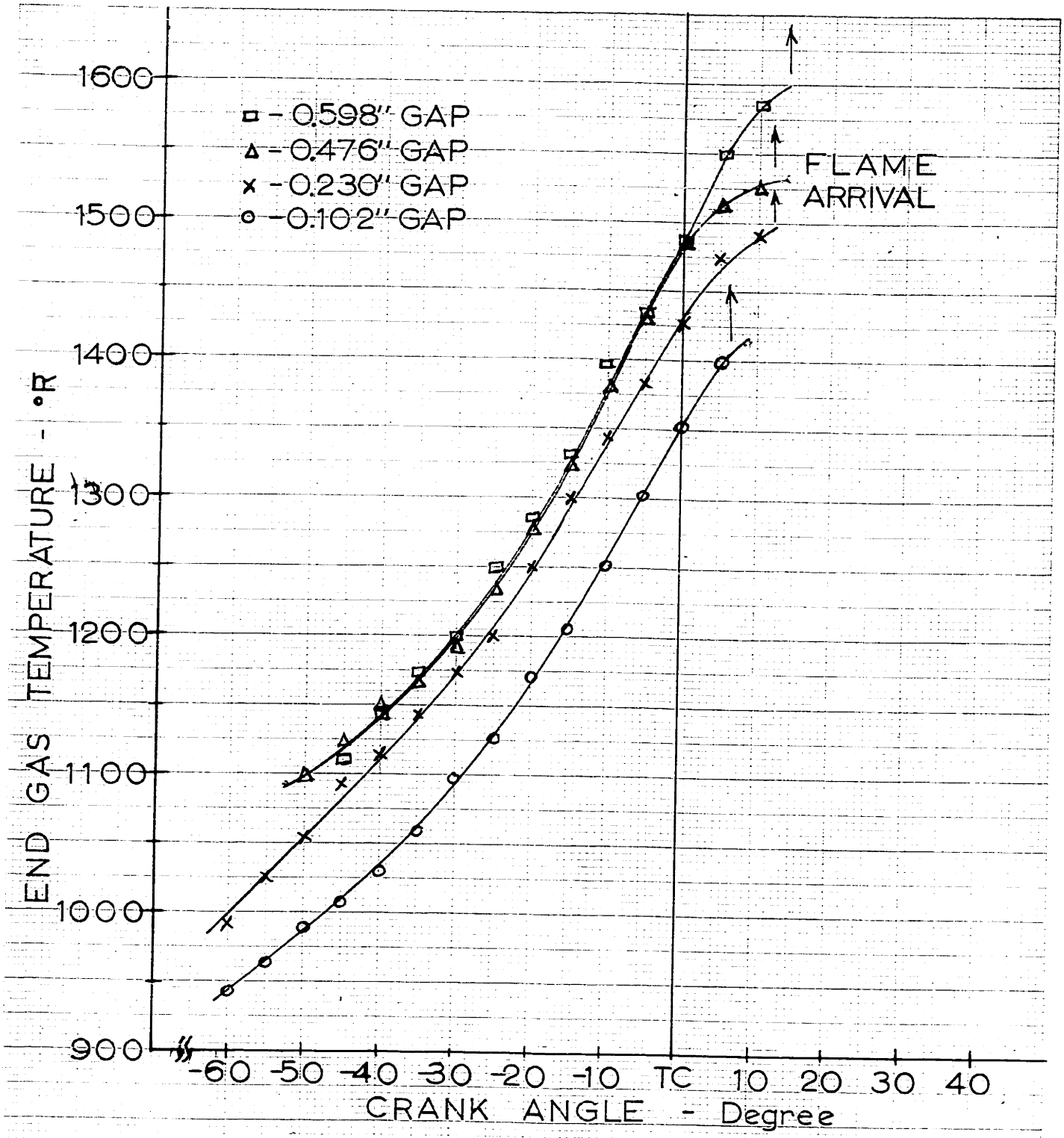

FIGURE 20 EFFECT OF GAGE LENGTH ON END GAS TEMPERATURE AT 2000 RPM FIRING

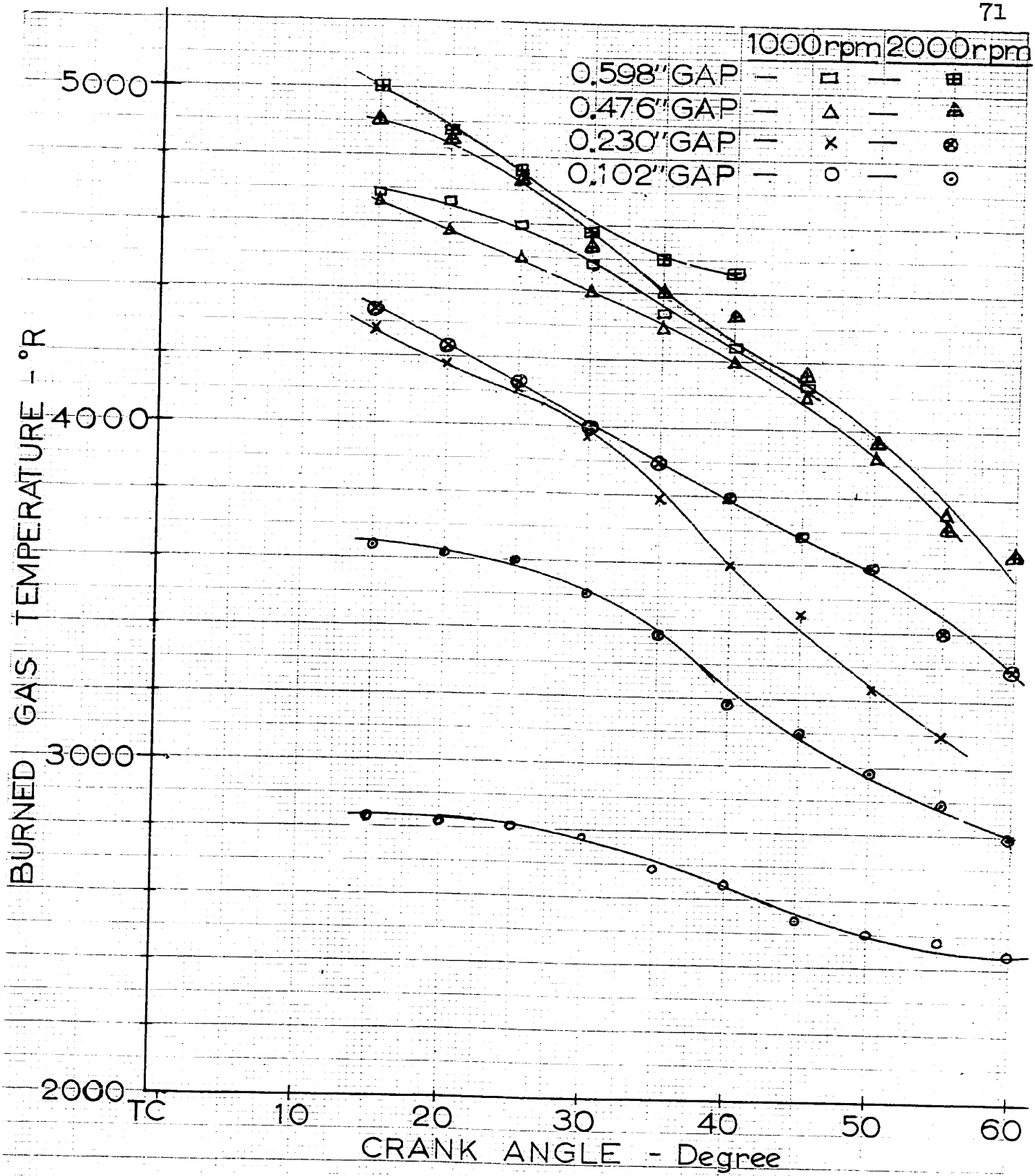

FIGURE 21 EFFECT OF GAGE LENGTH ON BURNED GAS TEMPERATURE

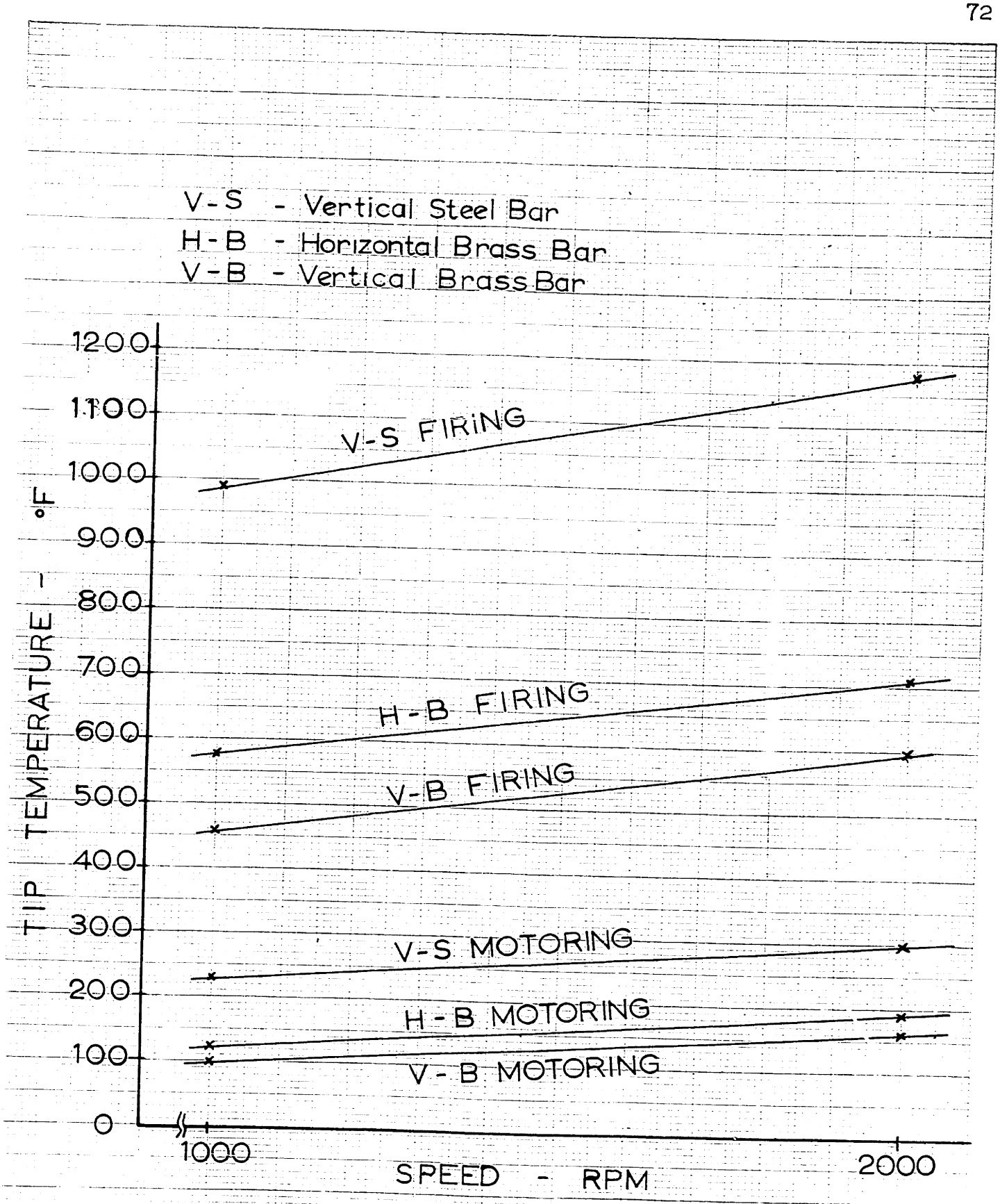

FIGURE 22 EFFECT OF TRANSDUCER BAR MATERIAL ON TIP TEMPERATURE

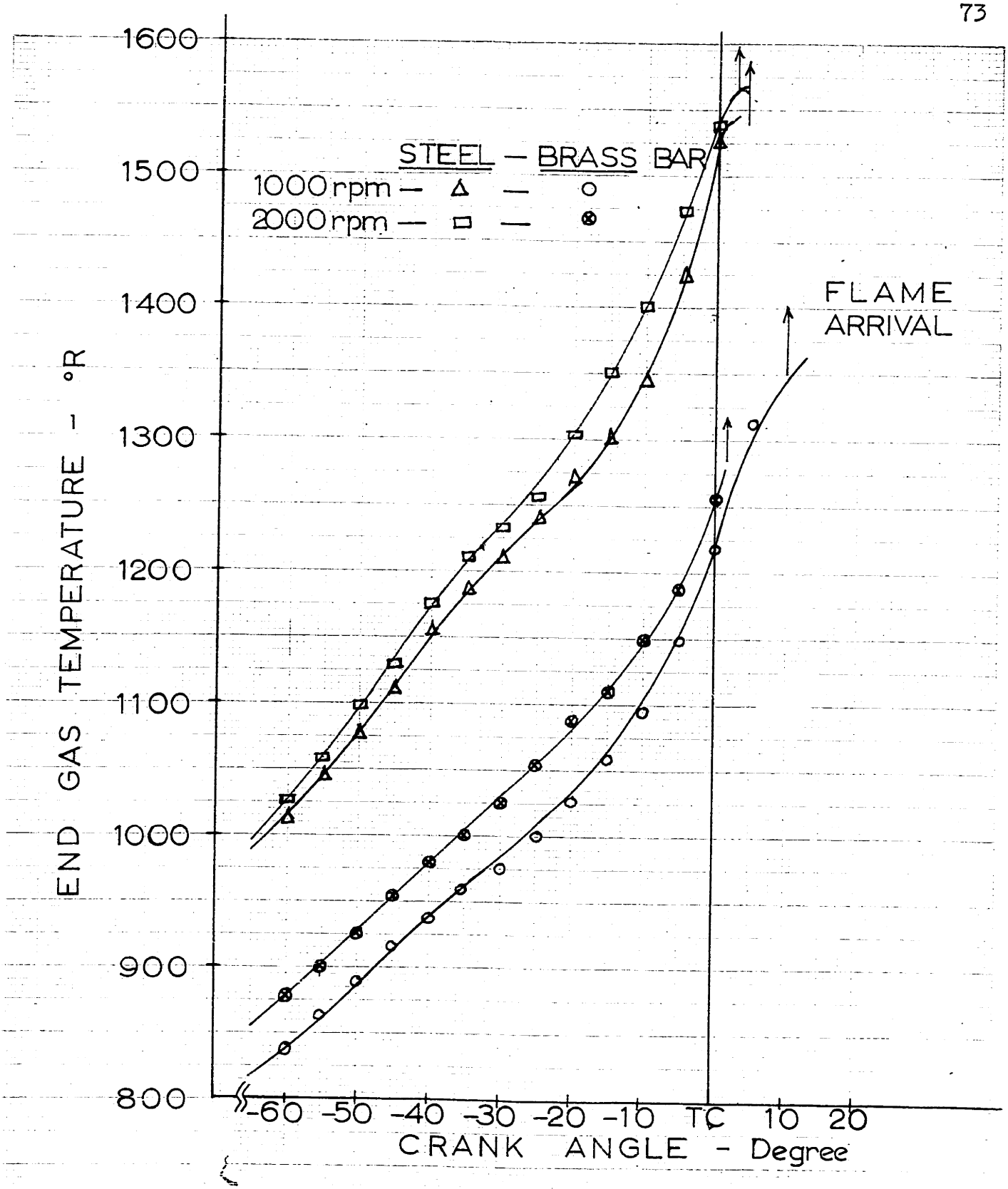

FIG. 23 EFFECT OF TRANSDUCER BAR MATERIAL AND SPEED ON END GAS TEMPERATURE AT FIRING

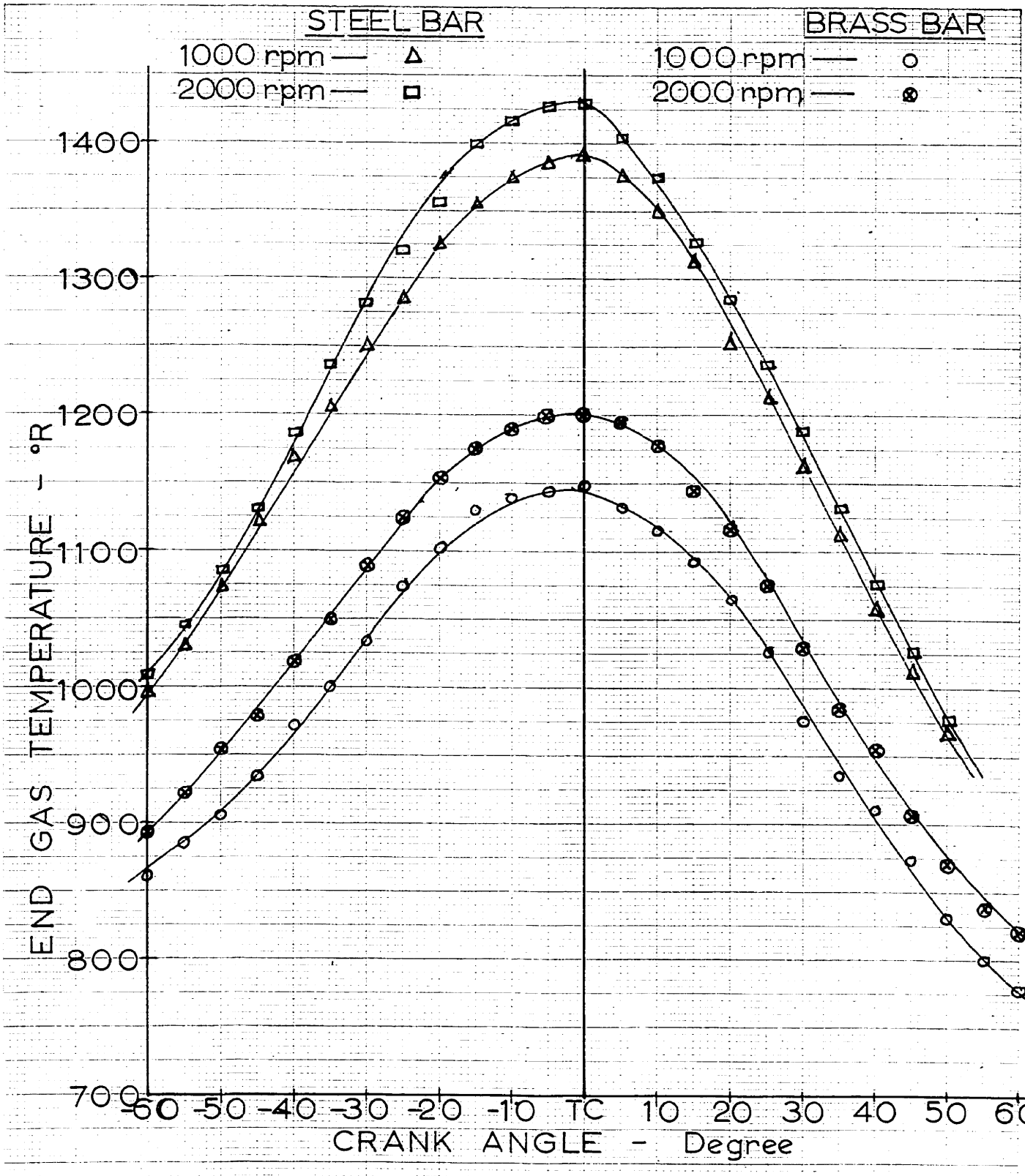

FIGURE 24 EFFECT OF TRANSDUCER BAR MATERIAL AND SPEED ON END GAS TEMPERATURE AT MOTORING

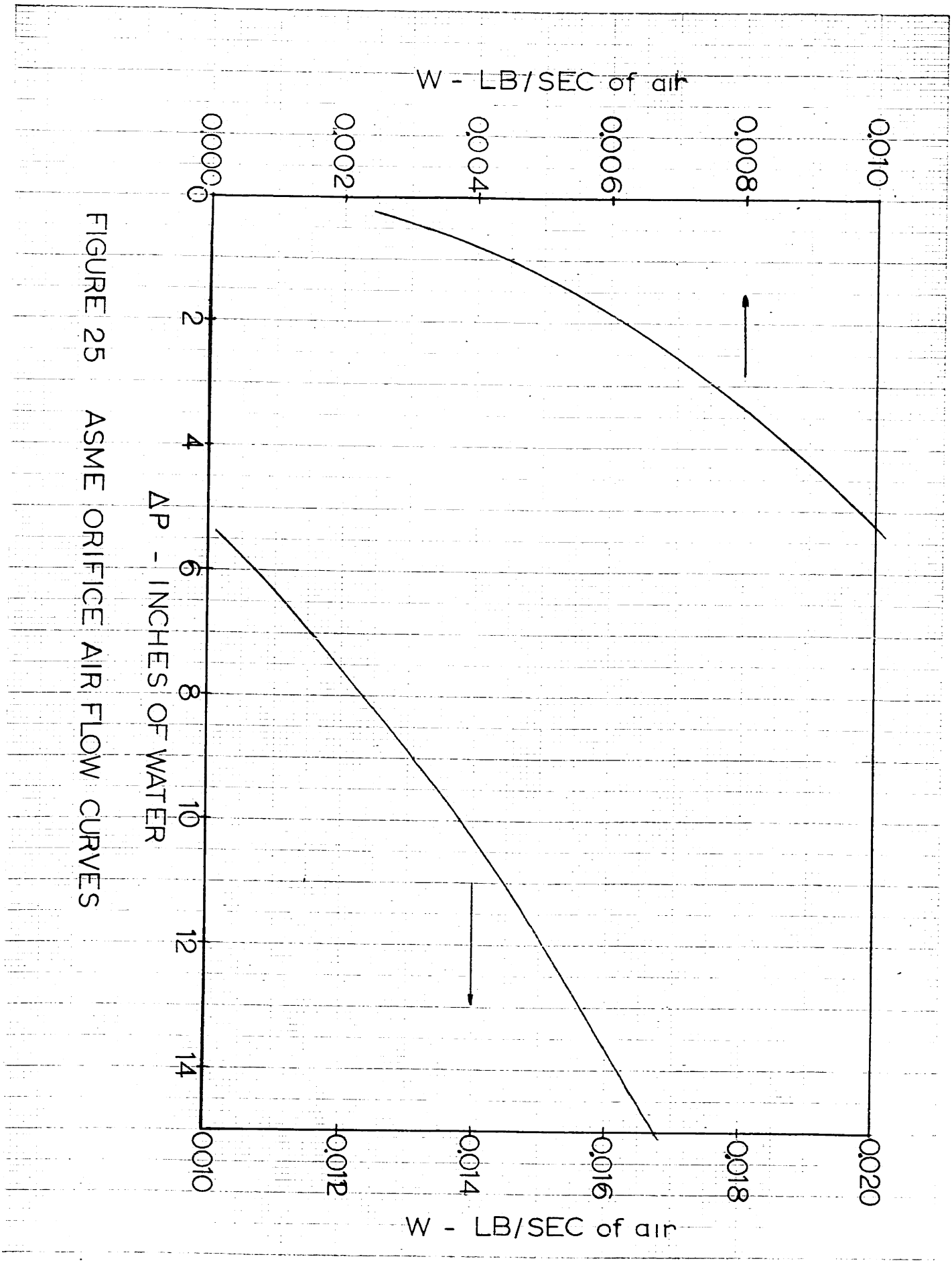

FIGURE 25 ASME ORIFICE AIR FLOW CURVES

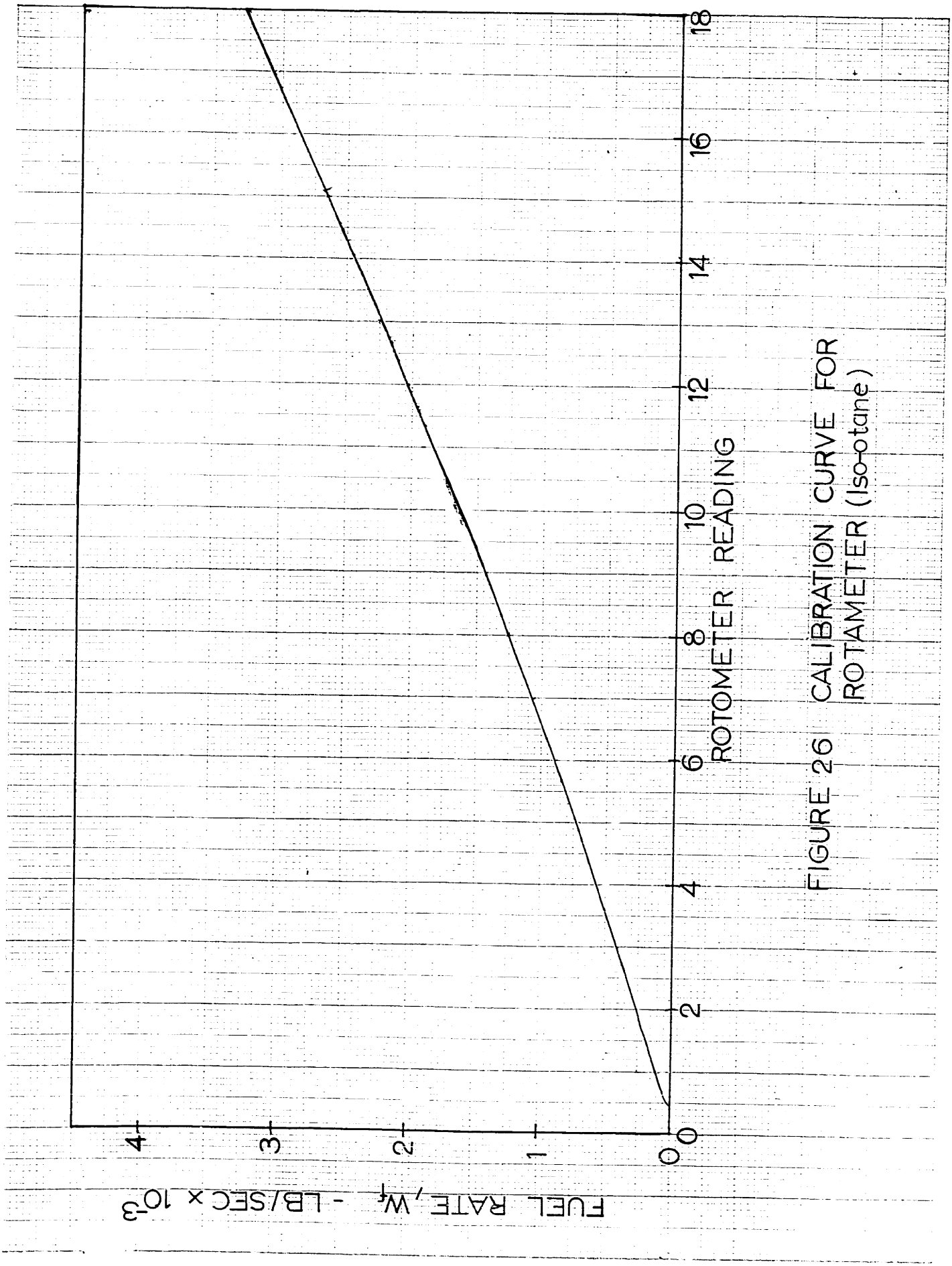

FIGURE 26 CALIBRATION CURVE FOR ROTAMETER (Iso-otane)